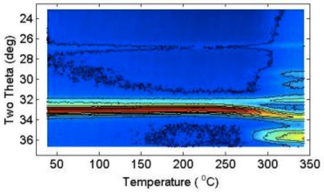

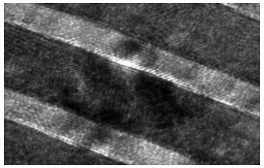

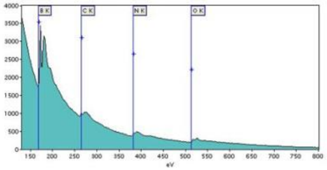

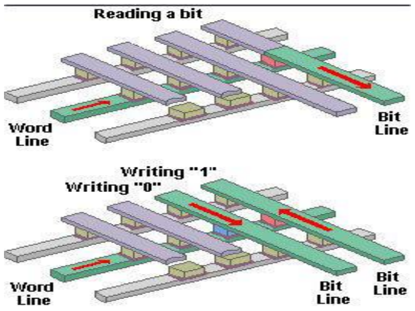

XRD/TEM/EELS Studies on Memory Device Structures

Santosh K. Kurinec
Electrical & Microelectronic Engineering
Rochester Institute of Technology
Rochester, NY 14623
Santosh.kurinec@rit.edu

Frontiers of Characterization and Metrology for Nanoelectronics (FCMN)
Dresden, Germany, April 14-16, 2015

Where is Rochester?

RIT

On Lake Ontario, one of the Great Lakes.

- Rochester is ~ 320 miles from NYC
- City population of ~250,000
- Six county area population of >1,000,000 people
- Strong Engineering and Business History
  - Eastman Kodak, Xerox, Bausch and Lomb
- 11 other colleges in the area
  - Totaling over 80,000 students

- Founded in 1829
- Privately endowed coeducational university
- 15,000 undergraduate and 3,000 graduate students
- More than 120,000 alumni world-wide

Strategically positioned for the growth of semiconductor industry in NY

Microelectronic Engineering @ RIT

Emphasis on semiconductor device design, process integration, Litho, DOE, SPC

Our 33 Years Moore's Law

Agenda

- Non Volatile Memory Technologies rely on a variety of Materials

- Need for Advanced Characterizations

- Two Type of Devices Investigated are Presented

    - Magnetic Tunnel Junction
    - Phase Change Memory Devices

Co-Authors

- Sankha Mukherjee, Showa Denko, Singapore
- Archana Devasia, NASA/GSFC, MD, USA
- Kris Campbell, Boise State University, Boise, ID, USA
- David MacMahon, Micron Technology Inc., Manassas, VA, USA
- Simone Raoux, Helmholtz-Zentrum Berlin für Materialien und Energie GmbH
- Jean Jordan-Sweet, IBM T. J. Watson Research Center, Yorktown Heights, NY, USA
- Surendra Gupta, RIT
- David Cabrera, Corning, NY, USA

Memory Devices

Volatile Memory

Non-Volatile Memory

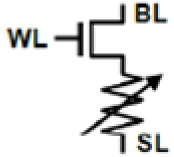

SRAM

DRAM

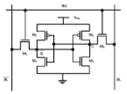

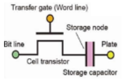

Charge Trap

Polarization change

Resistance Change

FLASH

SONOS

FRAM

PRAM

MRAM

RRAM

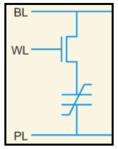

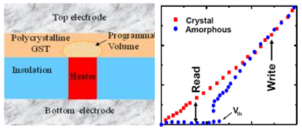

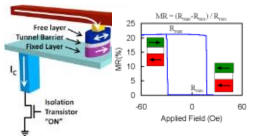

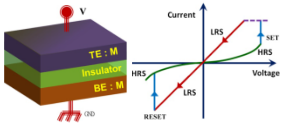

Charge based Programming & Reading

Current based Programming & Reading

Phase change causes resistance change

Magneto-resistance change

Interface or bulk resistance change

Moving electrons

Atom Movement

Electron Spin Movement

Ion Movement

Ref: Leti, June 2012, YOLE Développement

Magnetic Tunnel Junction in MRAM, STTRAM

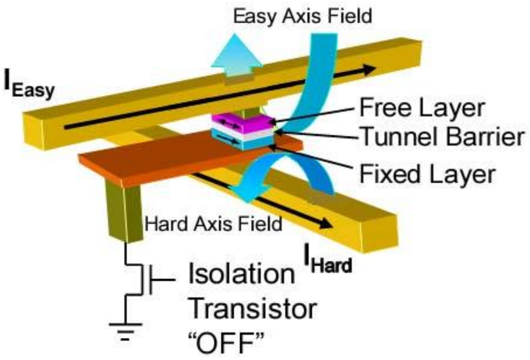

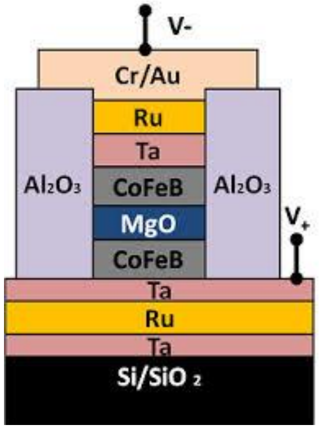

Phase Change Memory Cell

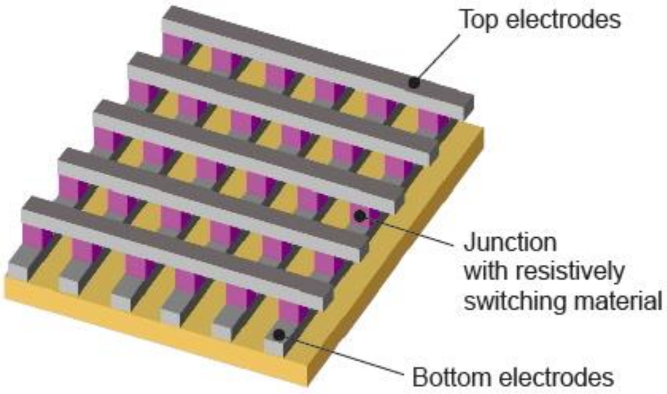

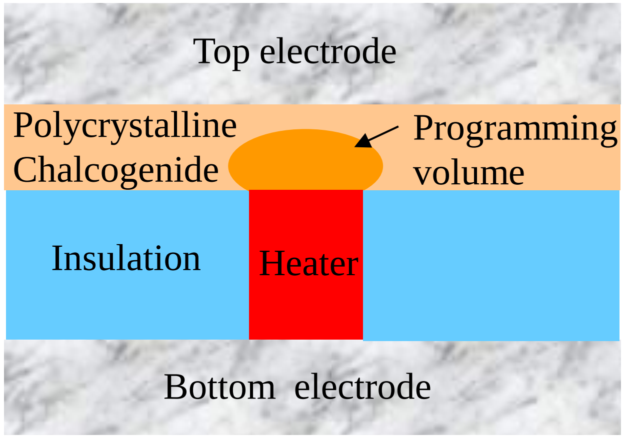

Crystallization and Inter-diffusion in nanoscale thin films plays a Huge role in their functioning

TEM/EELS & XRD

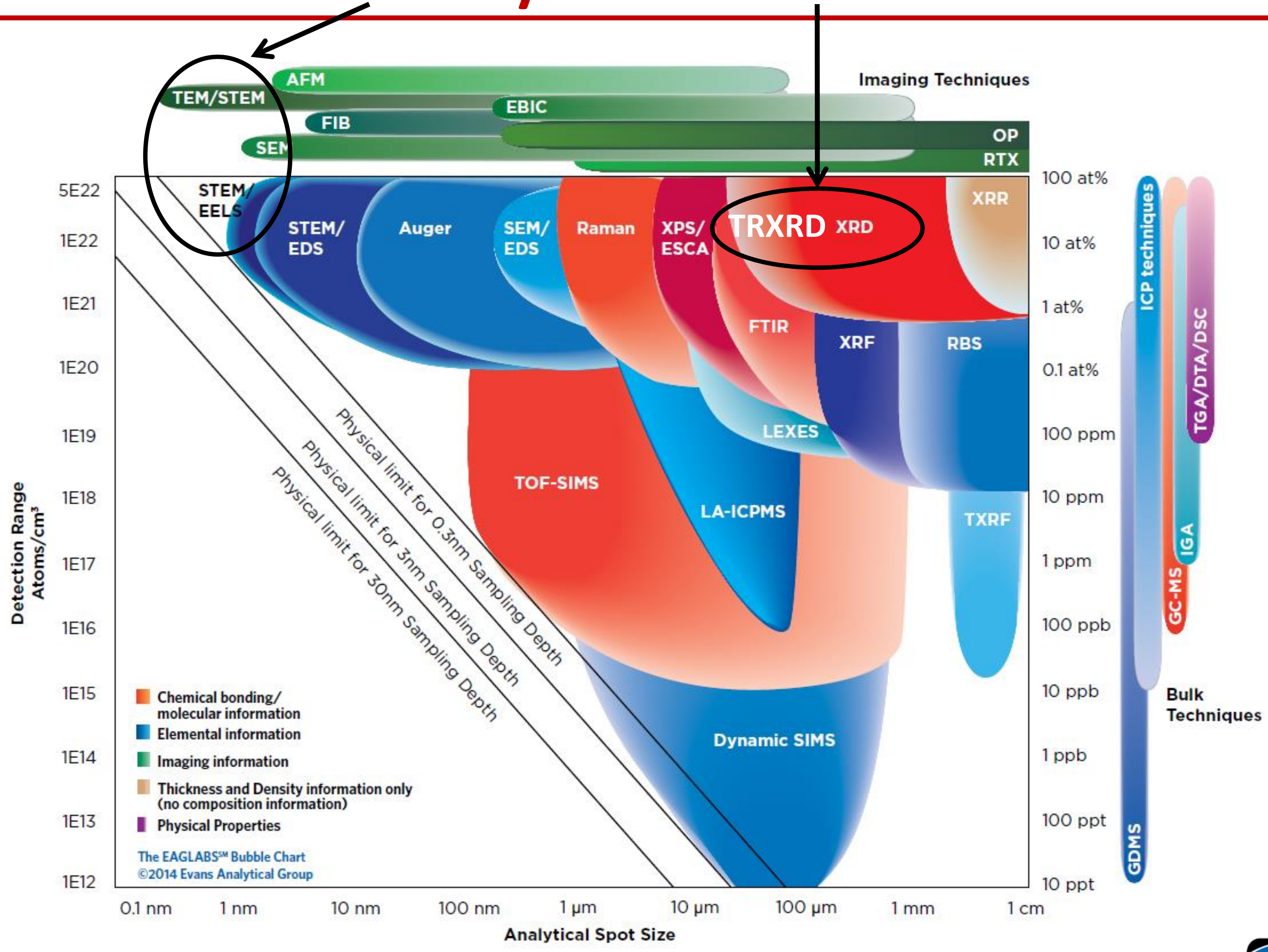
AFM
TEM/STEM
EBIC
FIB
OP
SEM
RTX
Imaging Techniques
TRXRD
STEM/ EELS
STEM/ EDS
Auger
SEM/ EDS
Raman
XPS/ ESCA
XRD
XRR
FTIR
XRF
RBS
LEXES
TOF-SIMS
LA-ICPMS
TXRF
Dynamic SIMS
Physical limit for 0.3nm Sampling Depth
Physical limit for 3nm Sampling Depth
Physical limit for 30nm Sampling Depth
ICP techniques
TGA/DTA/DSC
IGA
GC-MS
GDMS
Bulk Techniques
Detection Range Atoms/cm³
5E22
1E22
1E21
1E20
1E19
1E18
1E17
1E16
1E15
1E14
1E13
1E12
100 at%
10 at%
1 at%
0.1 at%
100 ppm
10 ppm
1 ppm
100 ppb
10 ppb
1 ppb
100 ppt
10 ppt
0.1 nm
1 nm
10 nm
100 nm
1 μm
10 μm
100 μm
1 mm
1 cm
Analytical Spot Size
Chemical bonding/ molecular information
Elemental information
Imaging information
Thickness and Density information only (no composition information)
Physical Properties
The EAGLABS℠ Bubble Chart
©2014 Evans Analytical Group

MTJ Design/Fabrication

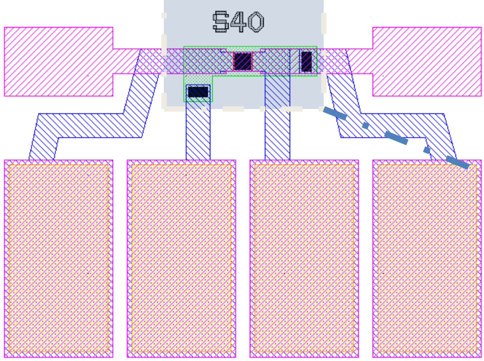

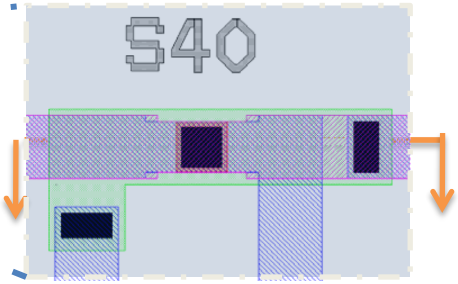

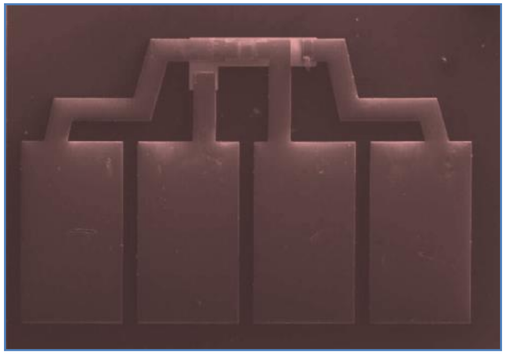

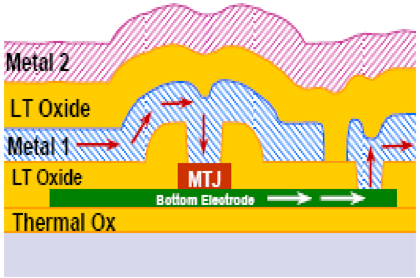

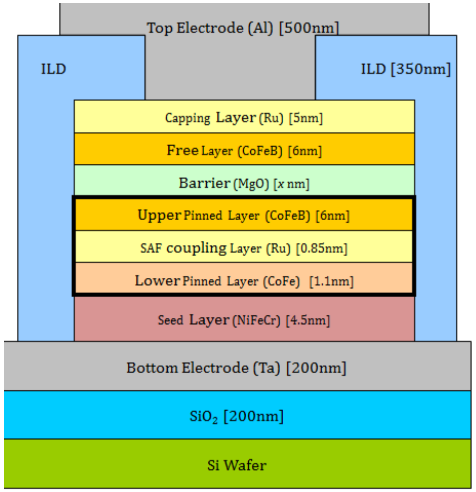

Top Electrode (Al) [500nm]

ILD

ILD [350nm]

Capping Layer (Ru) [5nm]

Free Layer (CoFeB) [6nm]

Barrier (MgO) [*x* nm]

Upper Pinned Layer (CoFeB) [6nm]

SAF coupling Layer (Ru) [0.85nm]

Lower Pinned Layer (CoFe) [1.1nm]

Seed Layer (NiFeCr) [4.5nm]

Bottom Electrode (Ta) [200nm]

SiO_2 [200nm]

Si Wafer

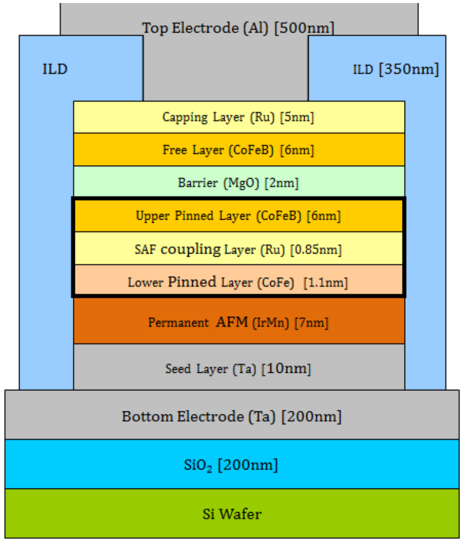

Top Electrode (Al) [500nm]

ILD

ILD [350nm]

Capping Layer (Ru) [5nm]

Free Layer (CoFeB) [6nm]

Barrier (MgO) [2nm]

Upper Pinned Layer (CoFeB) [6nm]

SAF coupling Layer (Ru) [0.85nm]

Lower Pinned Layer (CoFe) [1.1nm]

Permanent AFM (IrMn) [7nm]

Seed Layer (Ta) [10nm]

Bottom Electrode (Ta) [200nm]

SiO_2 [200nm]

Si Wafer

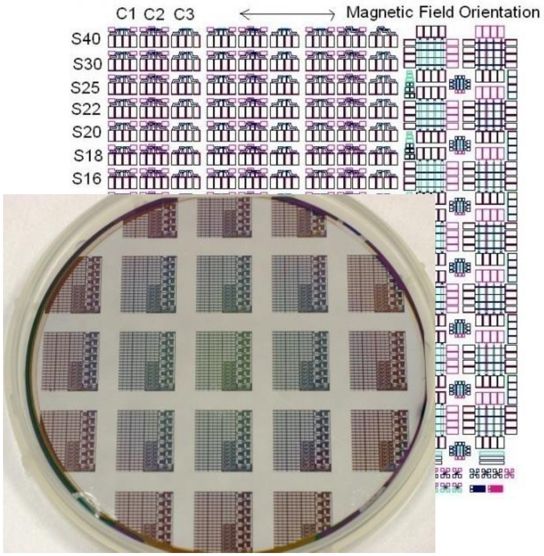

Deposited at Veeco using a multi-target sputter deposition system

Materials Characterization of Device Structures

Wide Range of Analytical Techniques Used in this Study

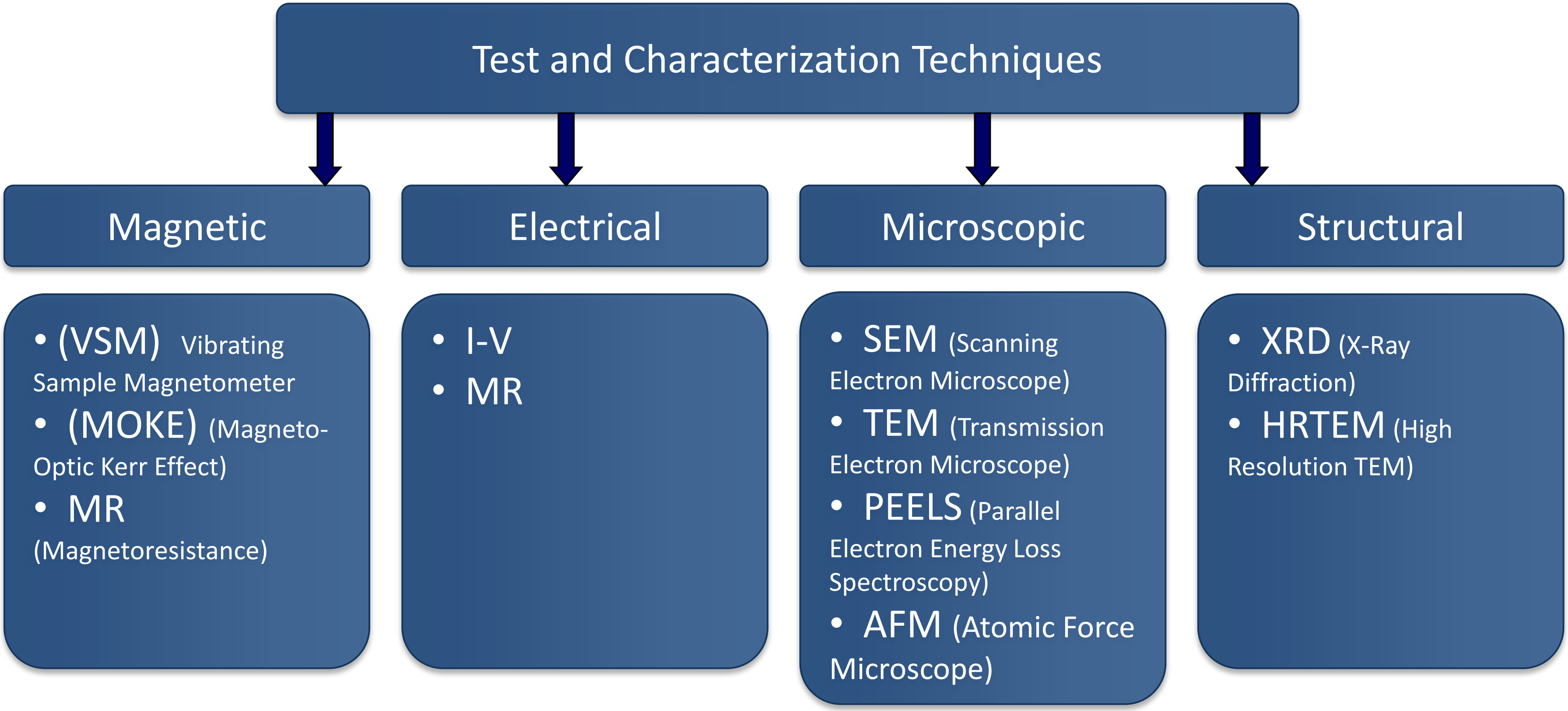

Test and Characterization Techniques

Magnetic

- (VSM) Vibrating Sample Magnetometer
- (MOKE) (Magneto-Optic Kerr Effect)
- MR (Magnetoresistance)

Electrical

- I-V
- MR

Microscopic

- SEM (Scanning Electron Microscope)
- TEM (Transmission Electron Microscope)
- PEELS (Parallel Electron Energy Loss Spectroscopy)
- AFM (Atomic Force Microscope)

Structural

- XRD (X-Ray Diffraction)
- HRTEM (High Resolution TEM)

- I-V, SEM, AFM, XRD at RIT
- VSM, MOKE at IBM
- TEM, PEELS at Micron
- MR at Cornell and NUS

Characterization
Electrical, Material,
Magnetic, …

Multilayer Structures Created to Study Crystallization

MgO
CoFeB
MgO
CoFeB
MgO
CoFeB
MgO
CoFeB
MgO
CoFeB
MgO
CoFeB
MgO
CoFeB
MgO
SiO_2 [200nm]
Si Wafer

Study of Crystallization, B migration

Material stack designed for materials analysis

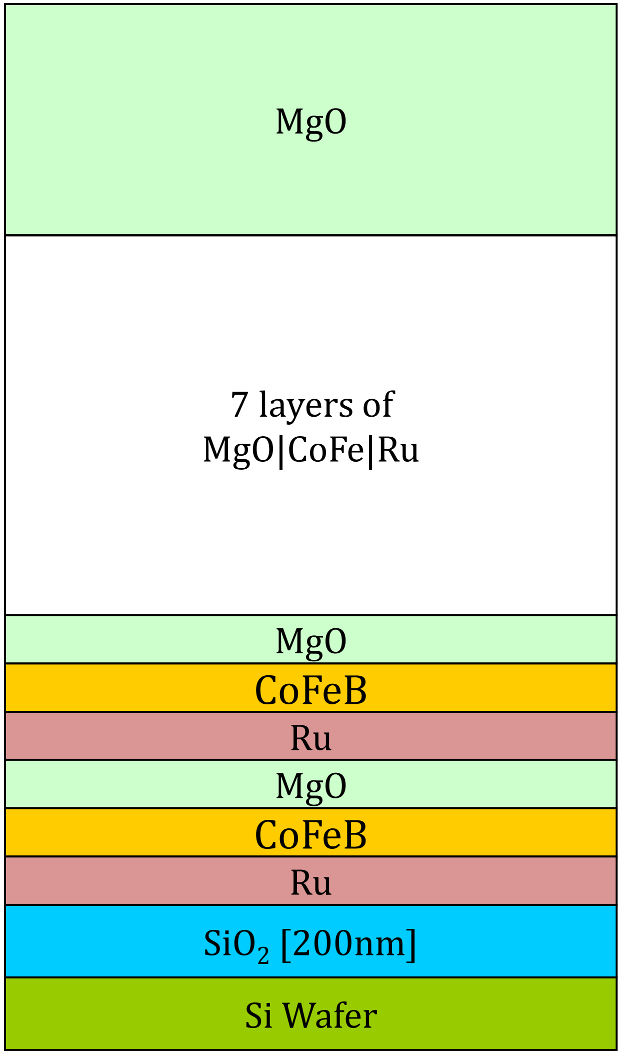

MgO
7 layers of MgO|CoFe|Ru
MgO
CoFeB
Ru
MgO
CoFeB
Ru
SiO_2 [200nm]
Si Wafer

Study of Inter-diffusion of Ru

Characterization Strategy

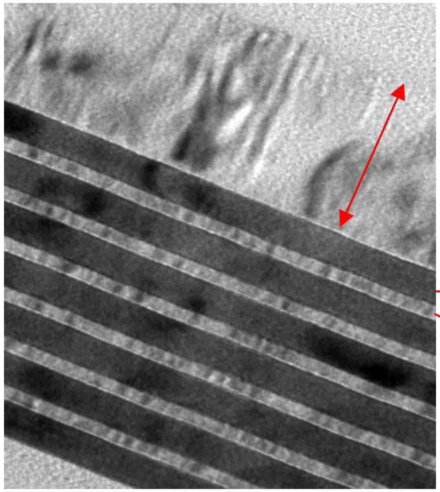

1. Study of B diffusion into MgO with Annealing
Methodology: TEM & PEELS

Diffusion monitor layer: MgO (25nm)

CoFeB (6nm)
MgO (2nm)

XRD^2 analysis layer: 7 layer stack

2. Study of the Crystallization Process with Annealing
Methodology: XRD^2 & TEM

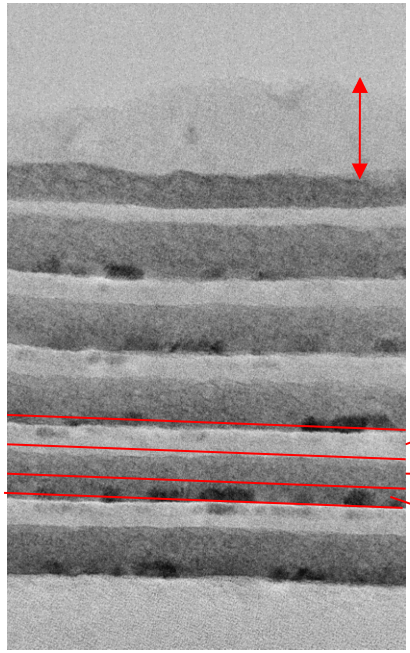

Diffusion monitor layer: MgO (25nm)

3. Study of Ru diffusion into MgO/CoFeB with Annealing
Methodology: TEM & PEELS

MgO (2nm)
CoFeB (6nm)
Ru (2nm)

XRD^2 analysis layer: 7 layer stack

3. Study of the **Crystallization Process** with Annealing
Methodology**: XRD^2 & TEM**

Study of Crystallization, B migration

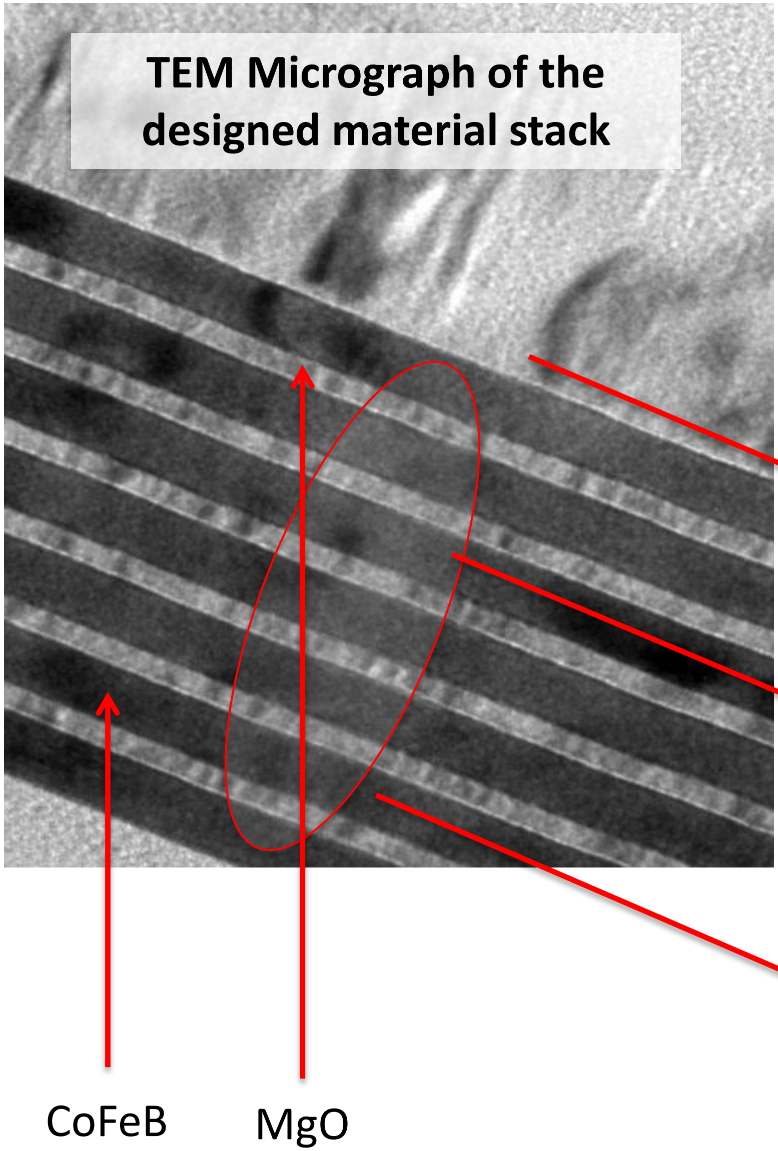
TEM Micrograph of the designed material stack

- Stacks are annealed at different temperatures
- 2D XRD performed to determine optimal process temperatures
  - (200) out-of plane MgO
  - (200) out-of-plane CoFe
- TEM performed to confirm crystallinity and structural integrity
- PEELS performed to determine elemental migration

Characterization of boron diffusion during anneal

Confirmation of structural integrity during the anneal

2D X-ray diffraction study of the crystallization of CoFe during annealing

2D XRD

Samples were annealed at various temperatures such as 250°C, 275°C, 350°C, 375°C, 385°C, 395°C, for 30min, and 60min.

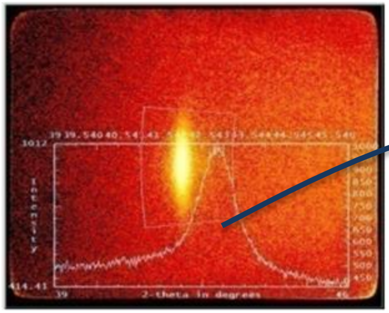

MgO (200)peak

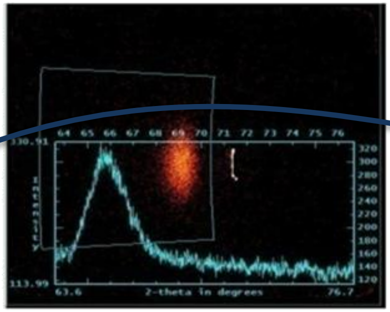

CoFe (200) peak

Gaussian Peak fitting

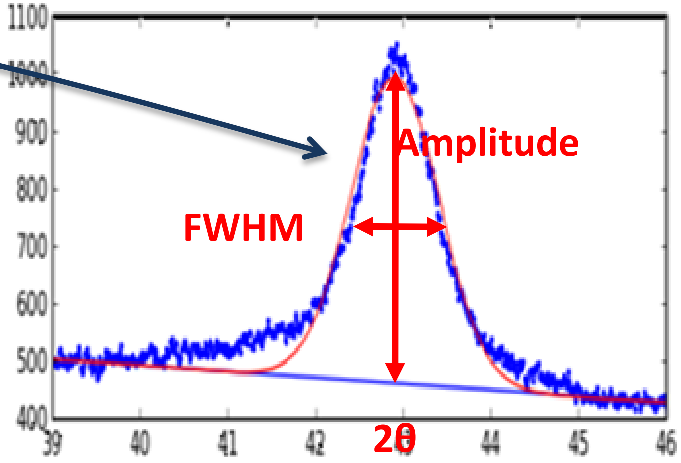

Peak fitting is done for every annealed sample and results are plotted as a function of anneal temperature

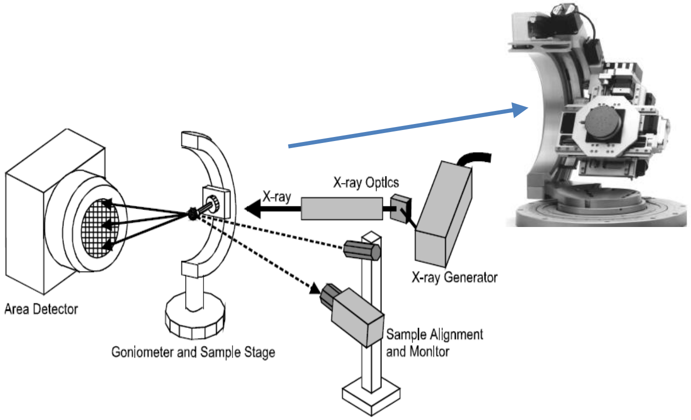

Bruker Dimension D8, with GADDS detector

Observations

1. As-deposited MgO is crystalline
2. Grain-growth is observed with increased anneal temperature
3. As-deposited CoFeB is amorphous
4. Crystallization of CoFeB begins at approximately 335°C. This also changes the slope of the 2θ change with temperature, corroborating the onset of CoFeB crystallization.

5. Increase in the CoFeB FWHM at 395°C is indicative of crystallographic degradation at that temperature.

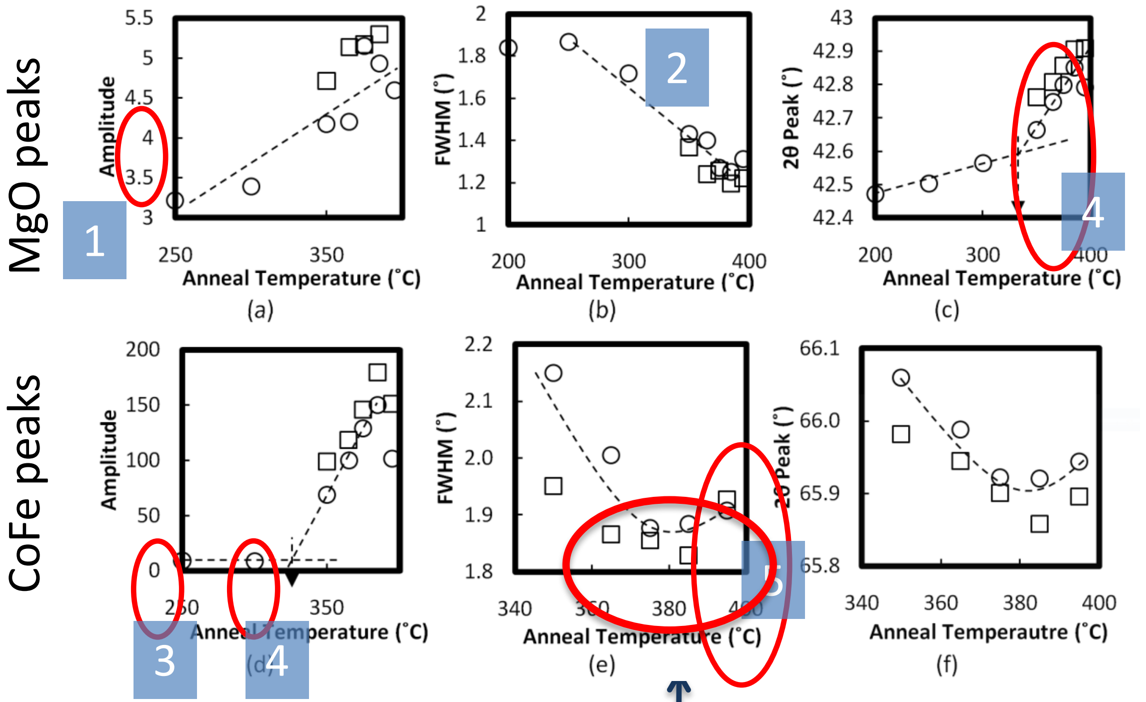

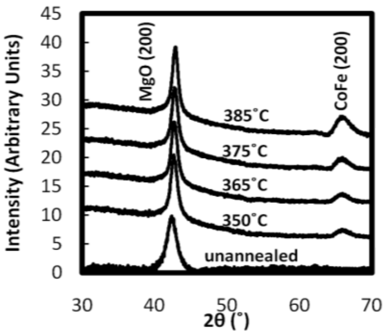

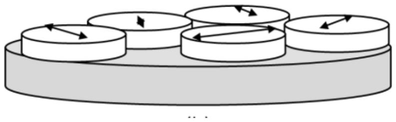

Multiple CoFe grains for every MgO grain

Process Window < 395°C

Samples on which TEM/PEELS performed: Unannealed, 350°C, 385°C, 395°C

Materials Characterization – TEM

High-resolution TEM Micrograph of the un-annealed sample

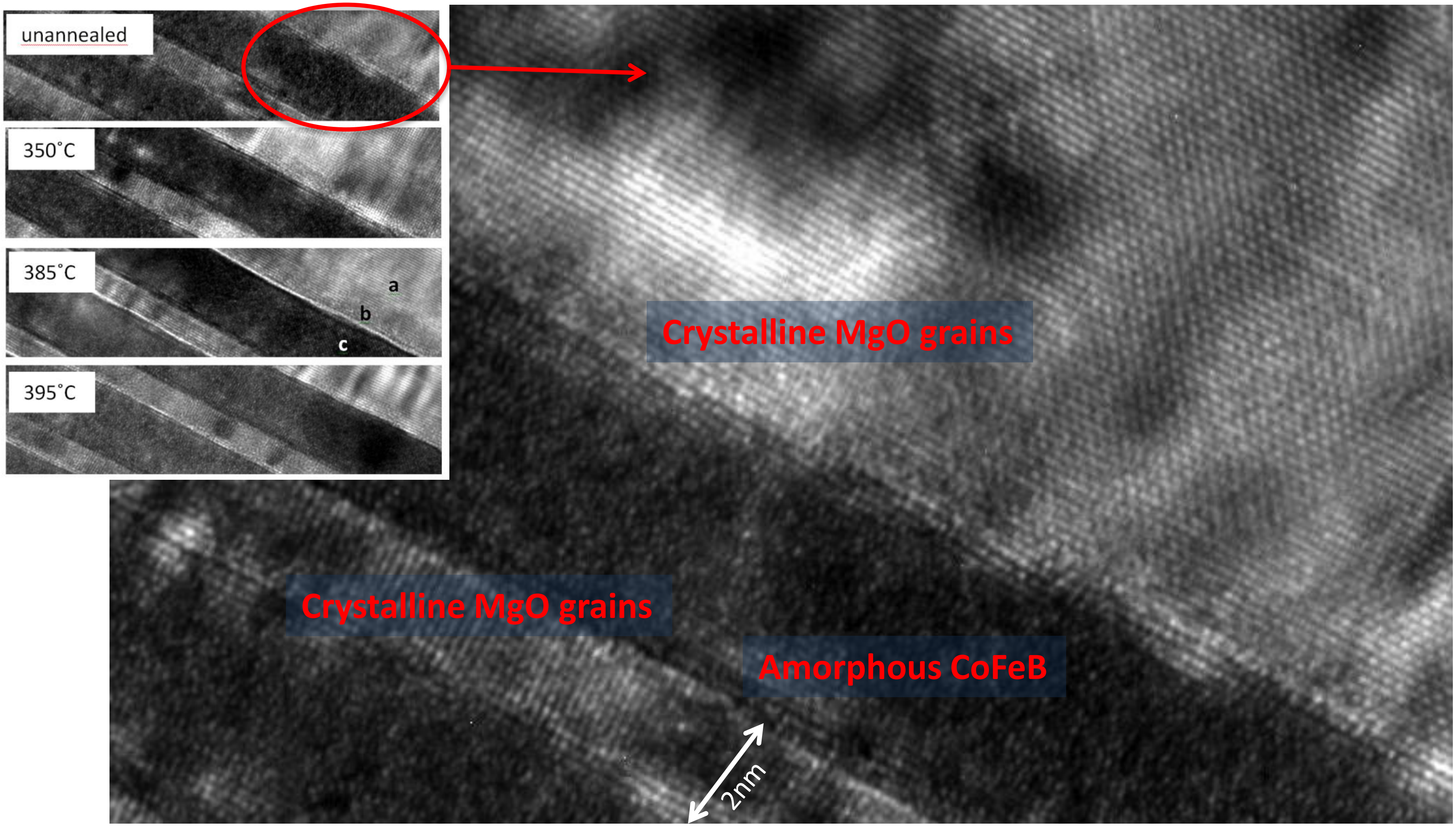

Materials Characterization – TEM

Beginning of Grain Formation

High-resolution TEM Micrograph of the sample annealed at 350°C

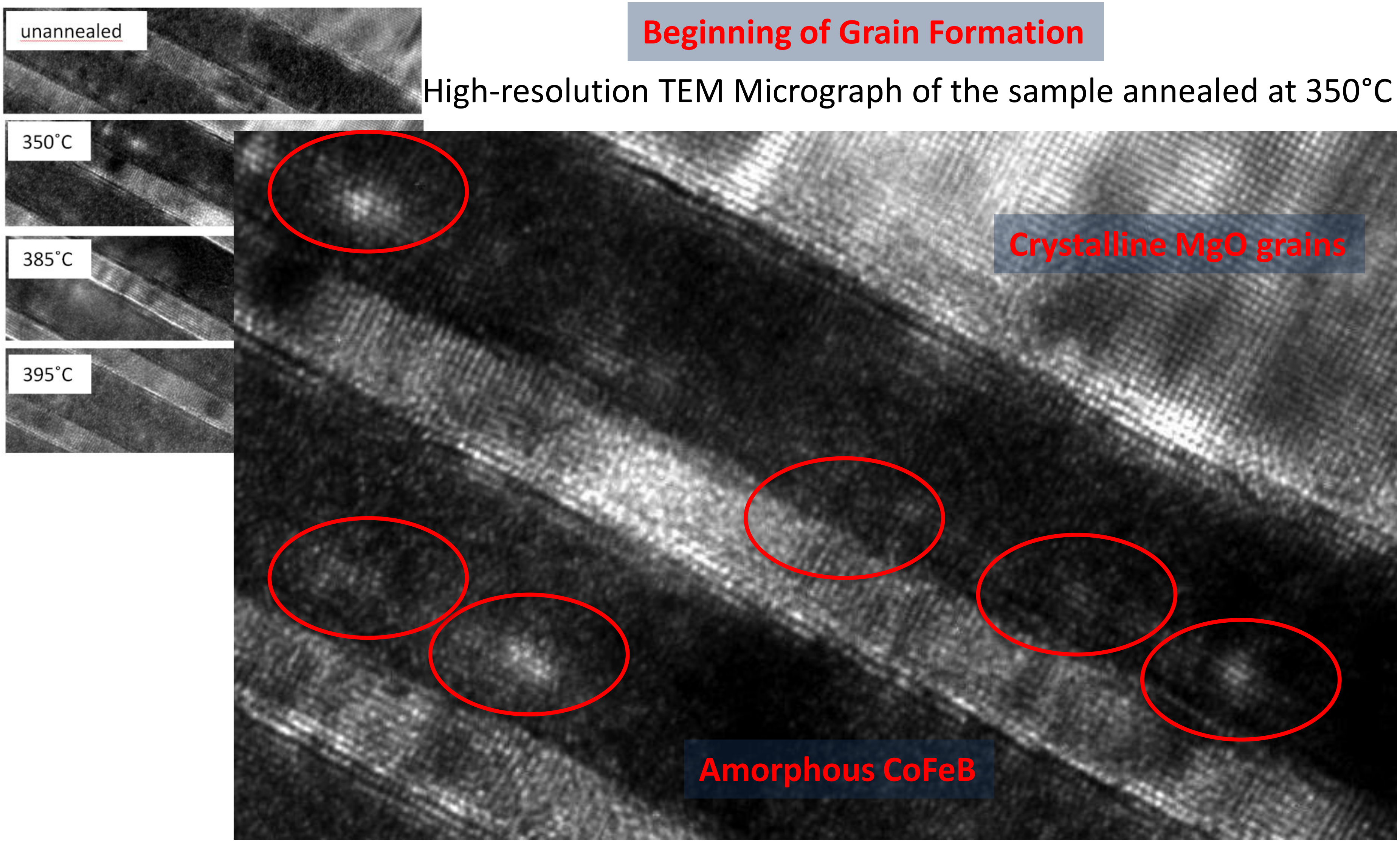

Materials Characterization – TEM

Significant Grain Formation

High-resolution TEM Micrograph of the sample annealed at 385°C

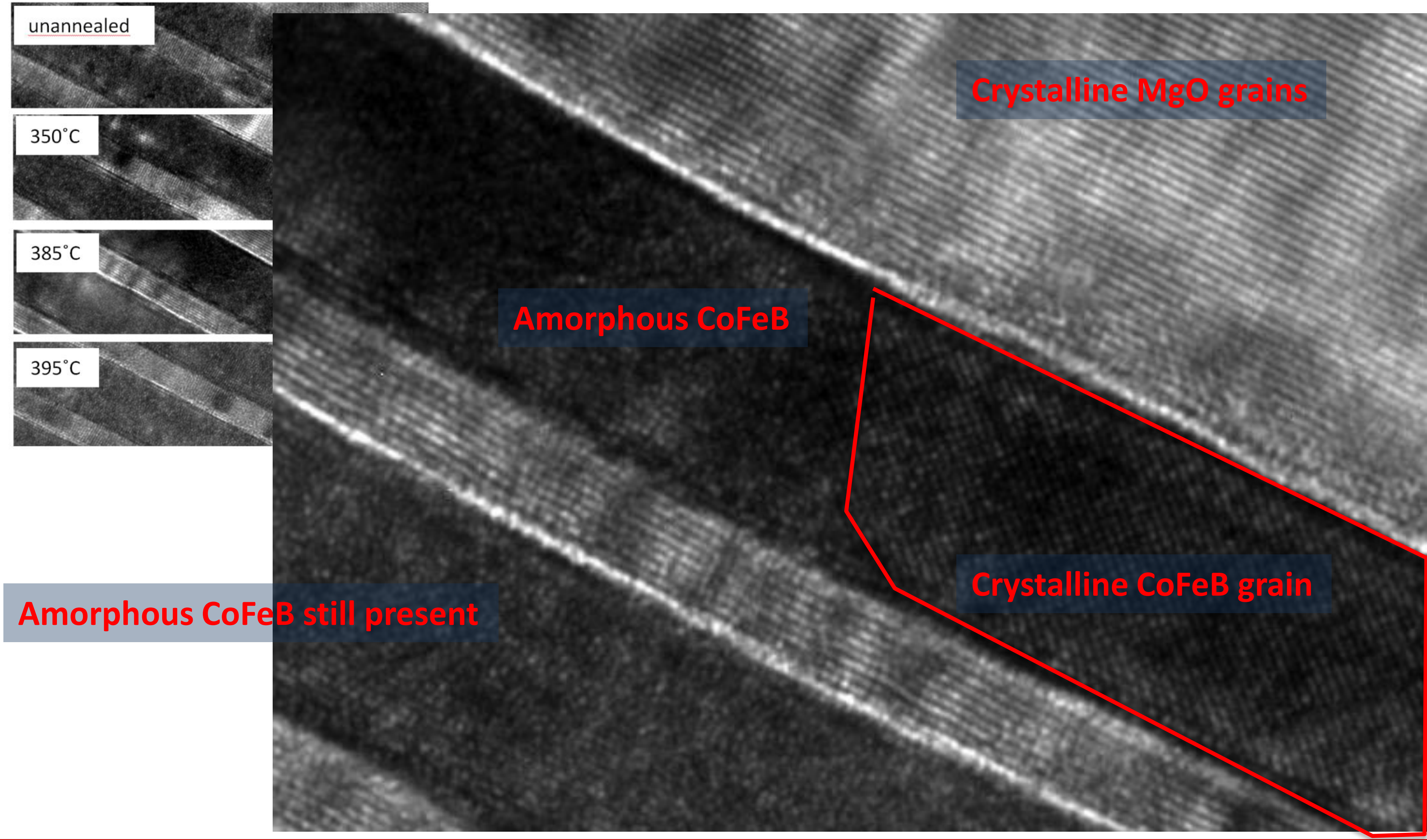

Crystalline MgO grains

Amorphous CoFeB

Crystalline CoFeB grain

Amorphous CoFeB still present

Materials Characterization – TEM

Anomalous Grain Formation

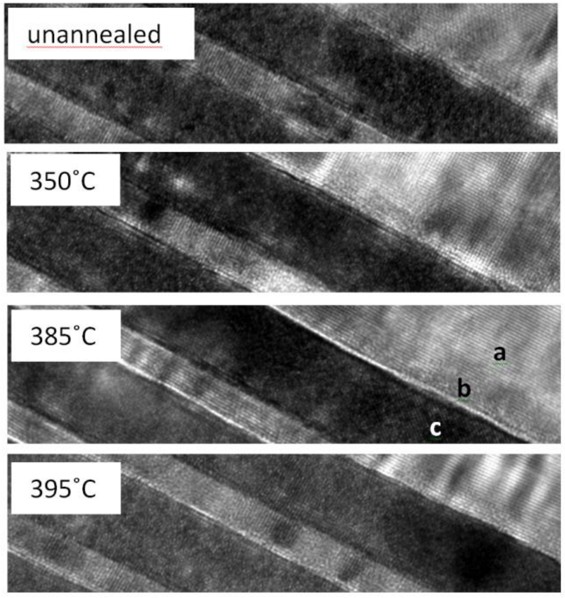

High-resolution TEM Micrograph of the sample annealed at 395°C

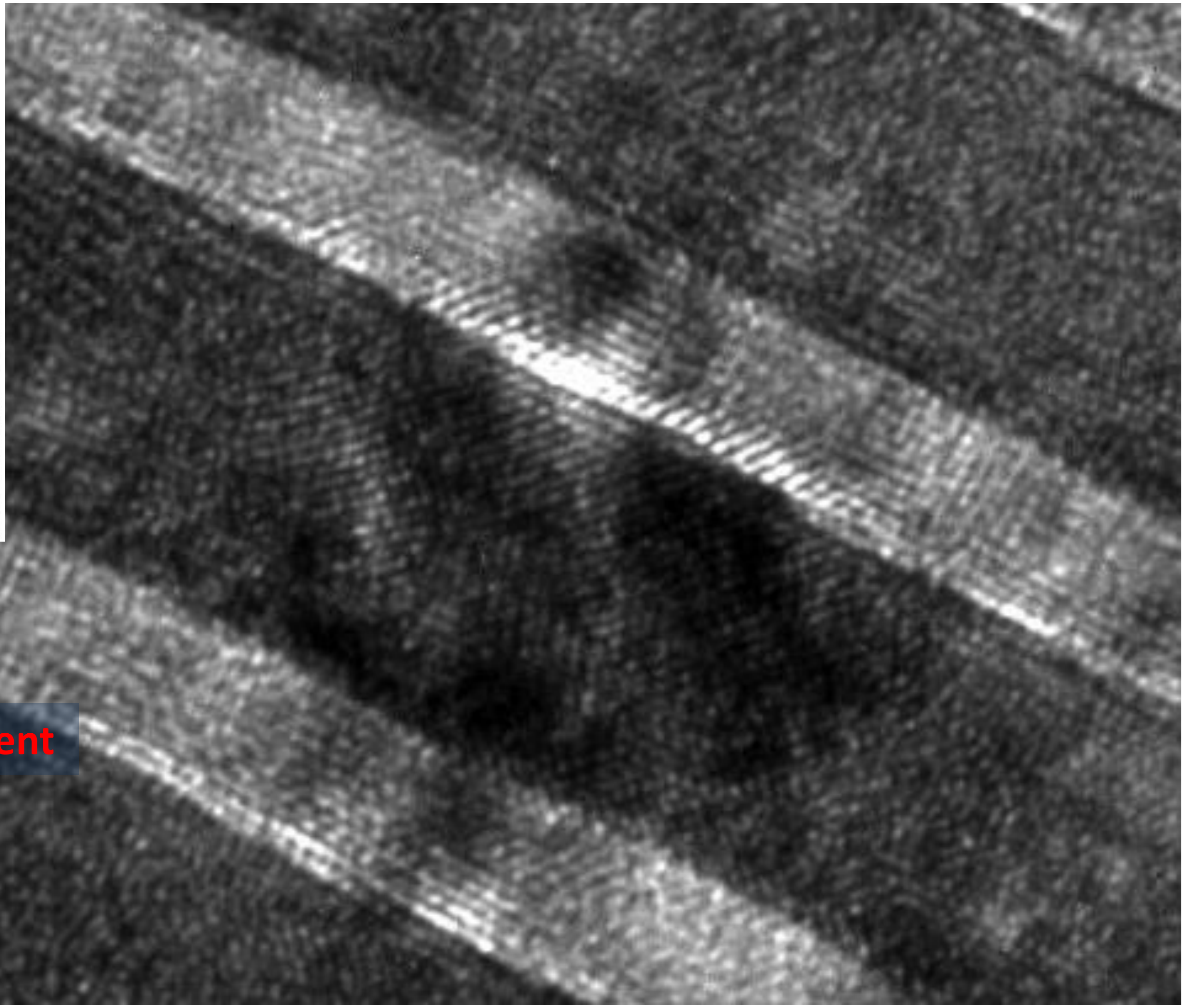

Amorphous CoFeB still present

TEM and PEELS

- PEELS is performed on 60 points along the line shown

0 refers to the first point, 59 refers to the last point , point-point spacing is 0.5Å

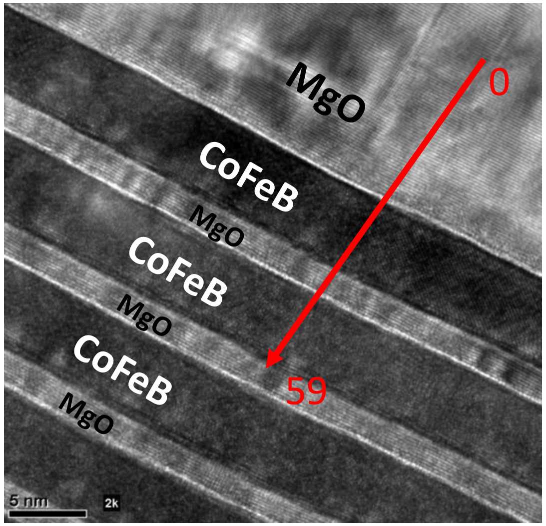

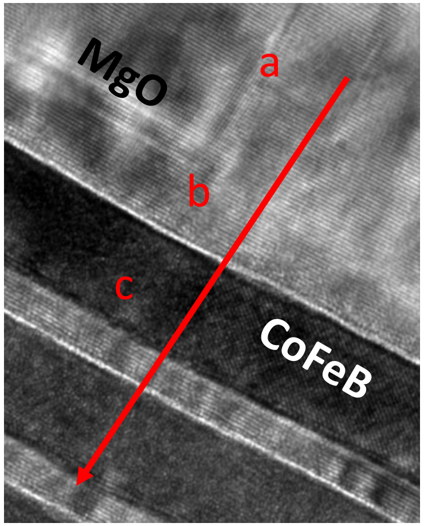

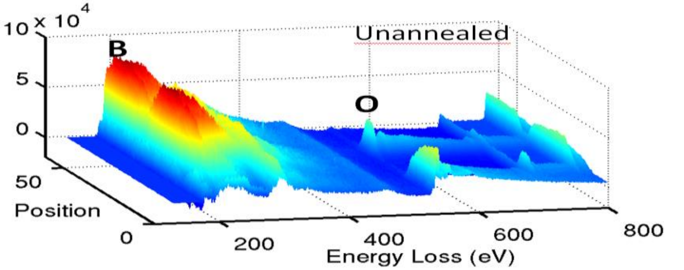

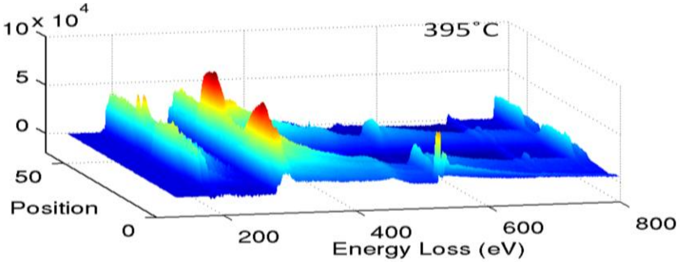

O spectrum

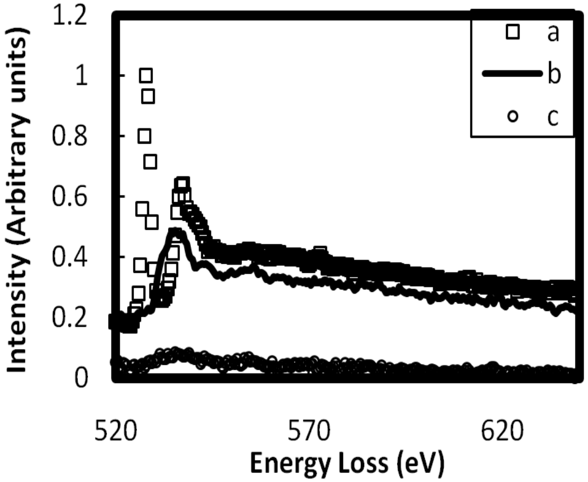

B spectrum

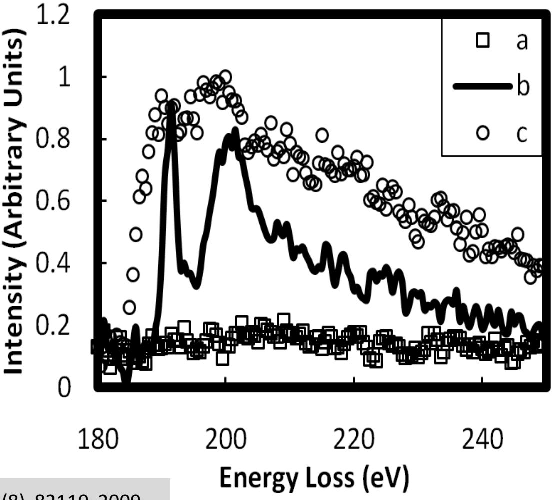

S. S. Mukherjee, *et al.*, *Appl. Phys. Lett.*, **94**(8), 82110, 2009.

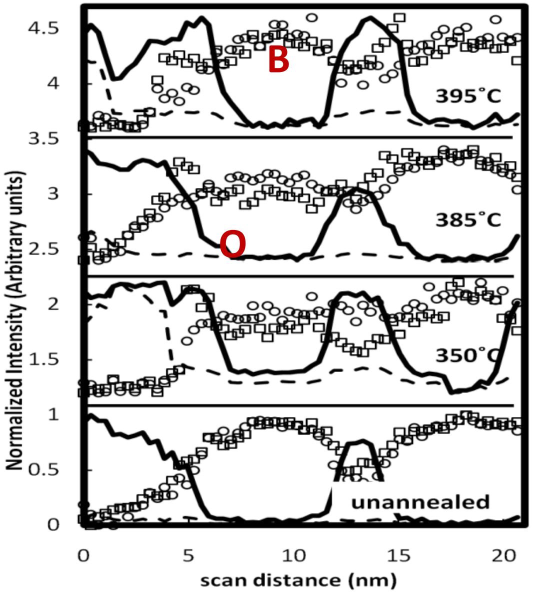

B spectrum

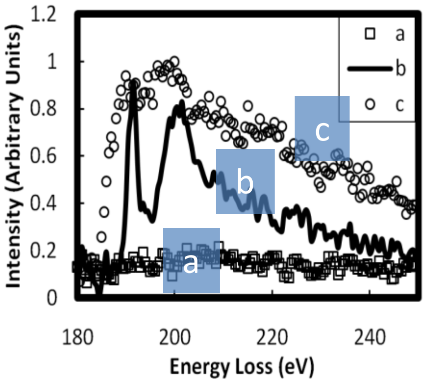

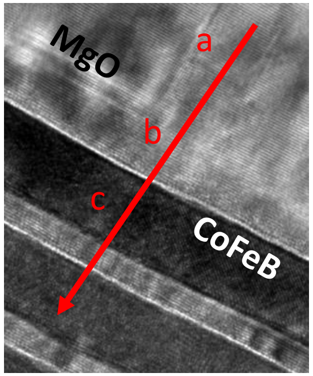

O spectrum

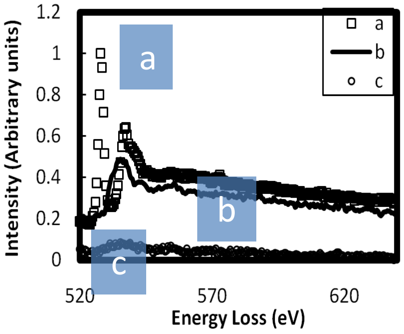

Energy-loss spectrum for B and O from three spatial positions are separated and plotted separately as shown above. These are marked by symbols ‘a’, ‘b’ and ‘c’.

○ **At ‘a’, there is no B** in the B spectrum, but O, as expected – B doesn’t penetrate deep into MgO.

○ It thus leads to the **possibility of quantifying diffusion** as a result of annealing.

○ **Bonding nature of B** significantly **different in** the CoFeB and MgO layers.

○ It leads to the possibility of **estimating** the **physical nature dictating B diffusion**.

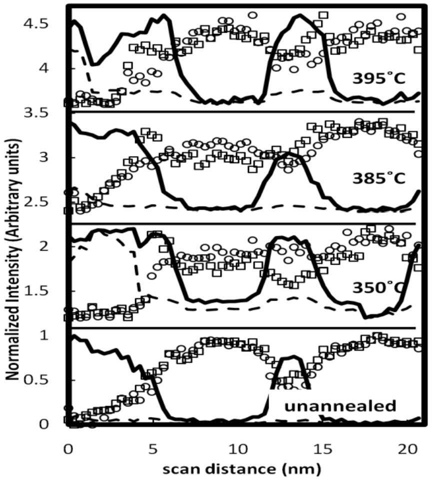

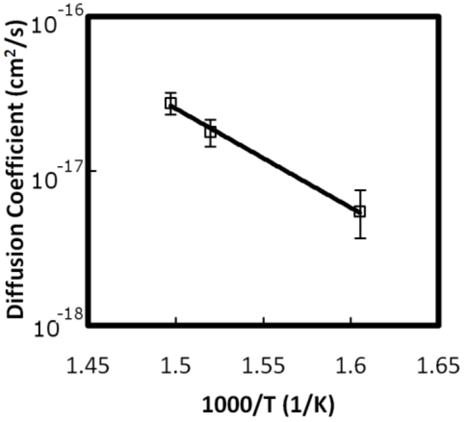

$$D = D_0 \exp\left(-\frac{E_A}{kT}\right)$$

$D_0 = 9.5\times10^{-8}\text{cm}^2/\text{s}$

$E_A = 1.3\pm0.4\text{eV}$

Materials Characterization – PEELS

395°C Anneal

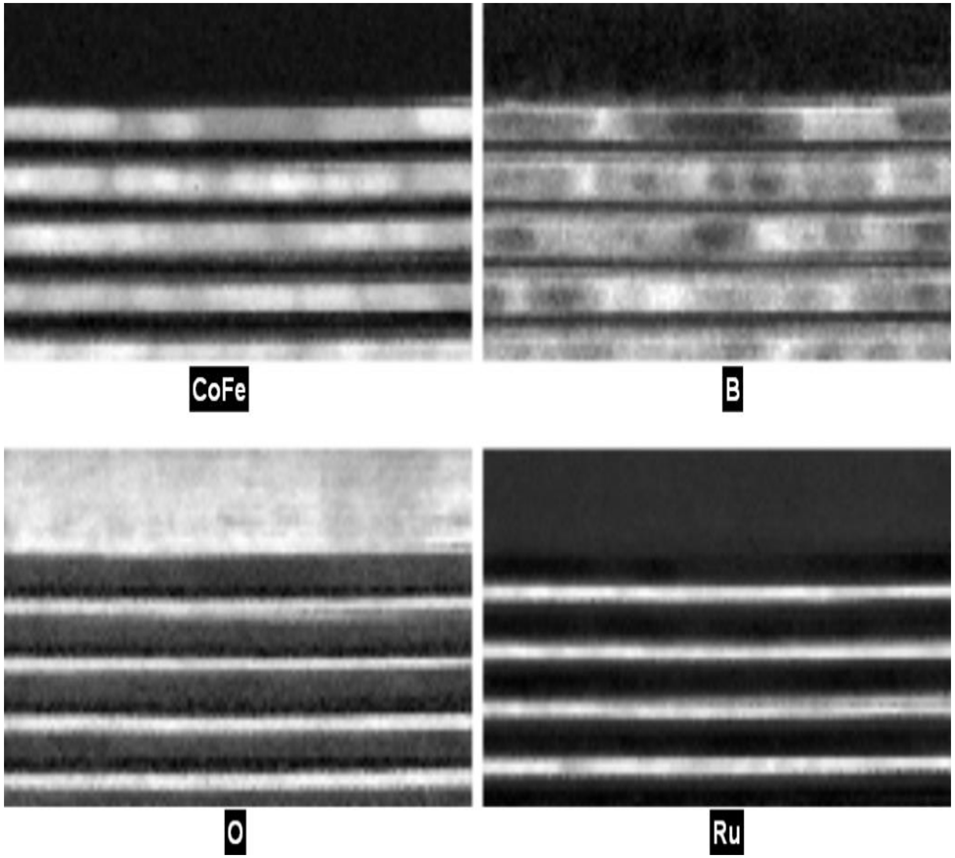

500°C Anneal

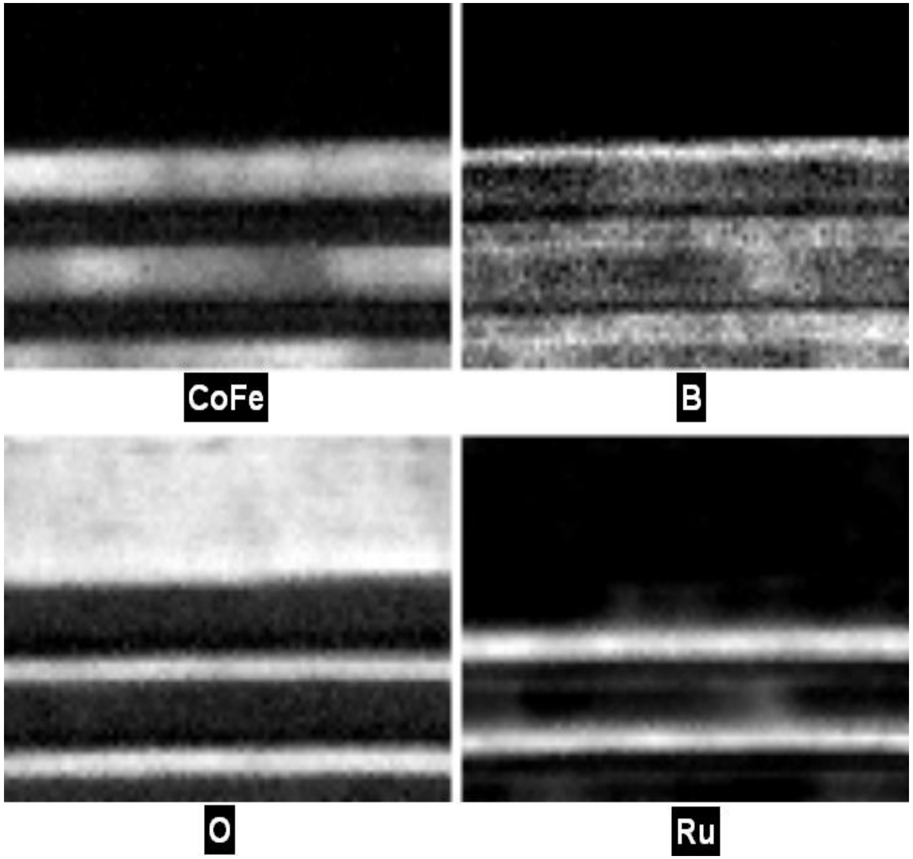

- **Ru does not interdiffuse at 395°C**, but does at 500°C
- B segregates not only vertically into the MgO, but also laterally into itself
- Ru diffuses into CoFeB, where there is high concentrations of B

What do we do with this Information?

Note: All current models assume fully-crystalline junctions

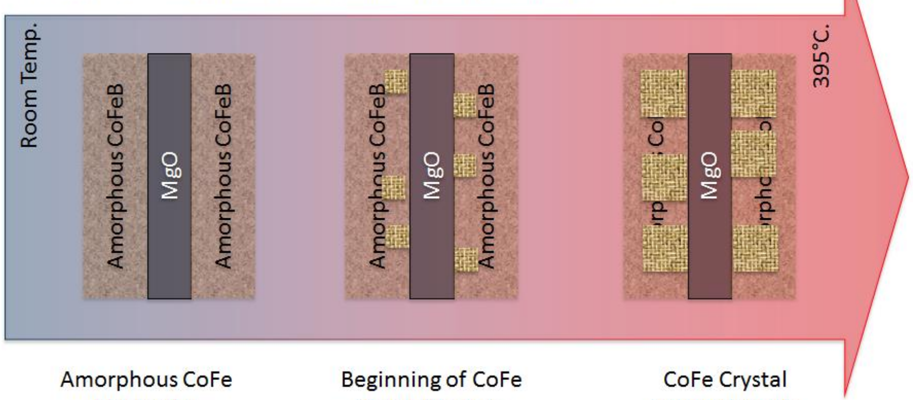

Amorphous CoFe Electrodes

Beginning of CoFe Crystallization

CoFe Crystal Grain-Growth

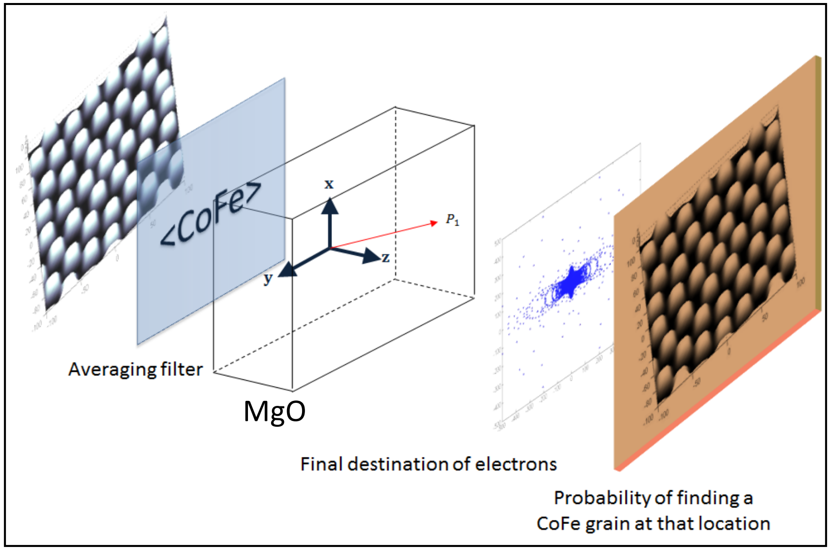

Grain Size dependence on tunneling magnetoresistance (TMR)

Improved Physical Model

TMR as a function of CoFe Grain size

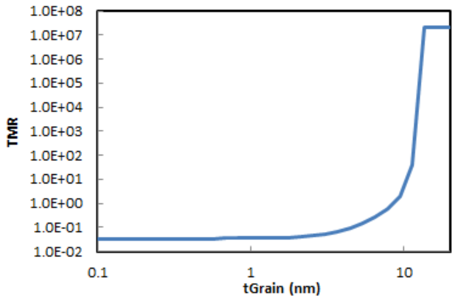

TMR as a function of barrier thickness

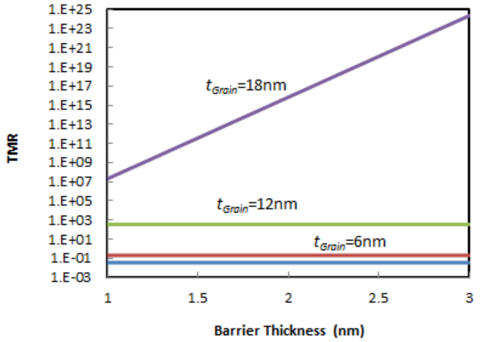

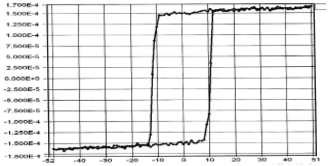

Hysteresis

- The TMR increases as a function of CoFe grain size
- For samples that are completely made of CoFe, there is a marked increase in the TMR as a function of distance.
- However, in the presence of any trace of CoFeB this increase is seen to disappear.

Phase Change Memory

- High bias, fast (10 ns pulse) melts chalcogenide
- Swift quench freezes material into amorphous, high resistance state

- Medium bias, 100 ns pulse heats chalcogenide to glass transition temperature
- Slow cooling nucleates and crystallizes into low resistance state

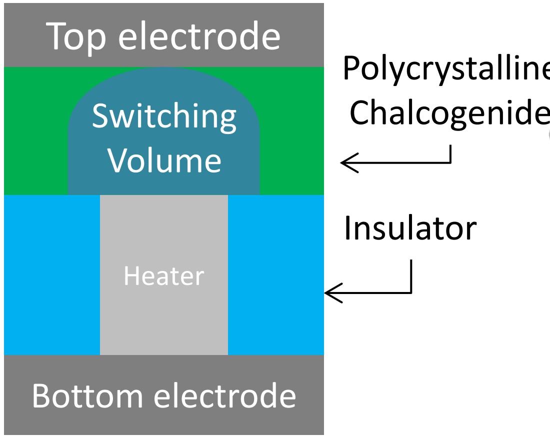

Top electrode

Switching Volume

Heater

Bottom electrode

Polycrystalline Chalcogenide

Insulator

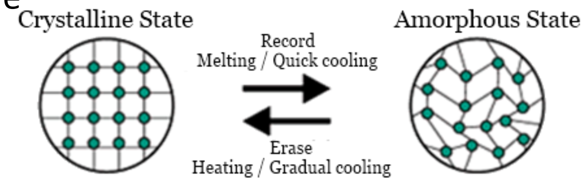

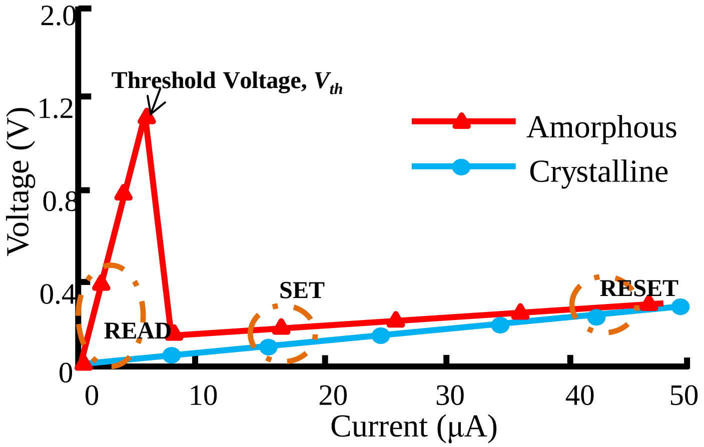

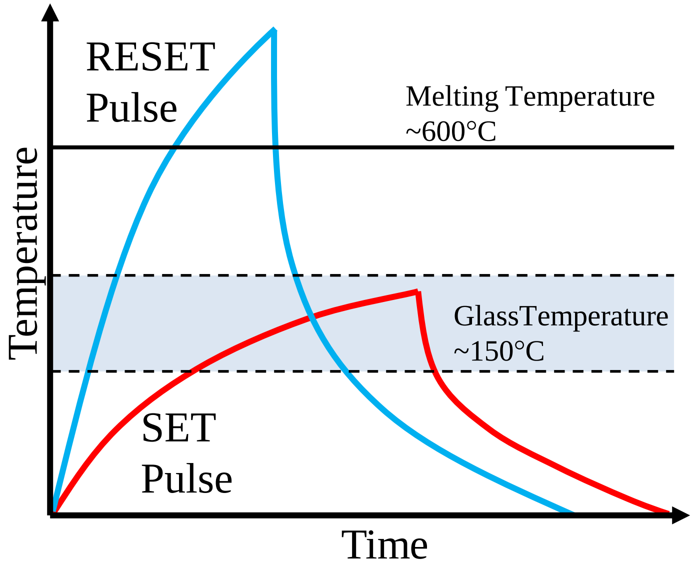

Stacked Chalcogenide Layers for Phase Change Memory

- **Bilayer Approach**
  - Bottom layer – Ge-Ch (GeTe or Ge_2Se_3)
  - Top Layer – Sn-Ch (SnTe or SnSe)

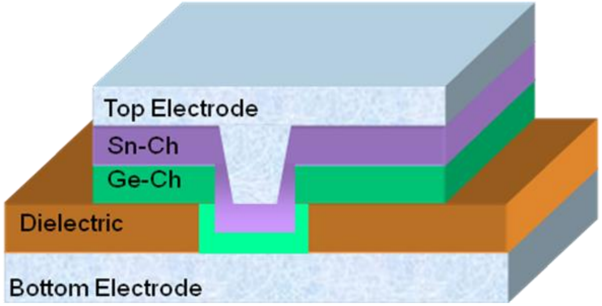

Device Schematic

- **Ge-Ch**
  - Homopolar bonds – nucleation sites
  - Ge_2Se_3 – higher T_G – higher temperature tolerance
- **Sn-Ch**
  - Ohmic contact
  - Improved adhesion
  - Donates metal ions
- Induce phase change response – possibility of lower V_{th} and current
- Tailor the characteristics of the memory layer
- Improve thermal cycling, reduce adhesion issues

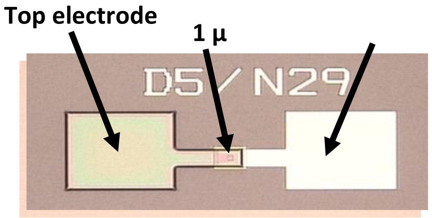

Fabricated device top view

Device Fabrication

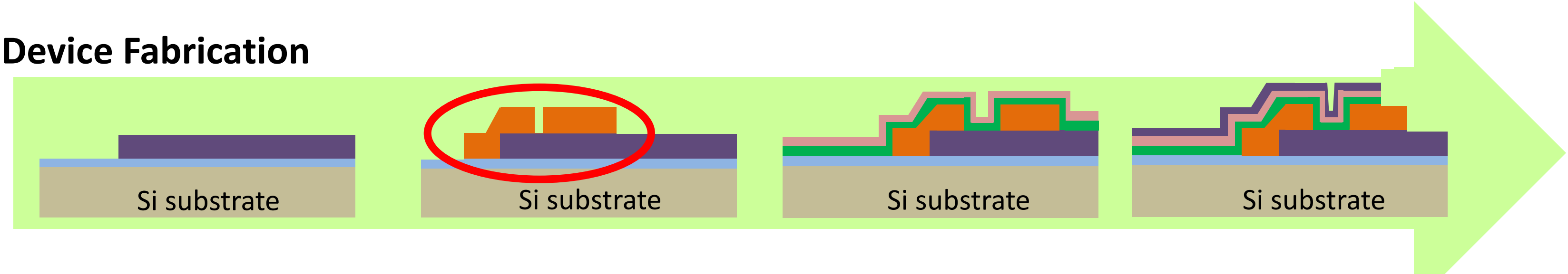

Level 2: Definition of Programming area and Sputter clean

Chalcogenide Evaporation

Level 3: Definition of Top Electrode

Phase Transition Studies and Residual Stress Analysis

- XRD carried out on bilayers of Ge_2Se_3/SnTe and GeTe/SnTe
- Cu Kα radiation, λ = 1.5418Å

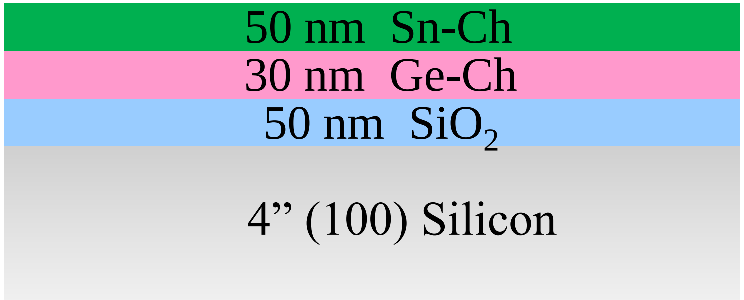

50 nm Sn-Ch

30 nm Ge-Ch

50 nm SiO_2

4” (100) Silicon

Bruker D8 HRXRD at RIT Advanced Materials Characterization Lab

Vantec 2000 Area Detector

- Samples heated in an Anton-Paar DHS900 domed hot stage to different annealing temperatures under flowing N_2 @ 30˚C/min, held for 10 min and cooled at the same rate

Ge_2Se_3/SnTe Bilayer

Amorphous Ge_2Se_3

Crystalline SnTe PDF# (046-1210)

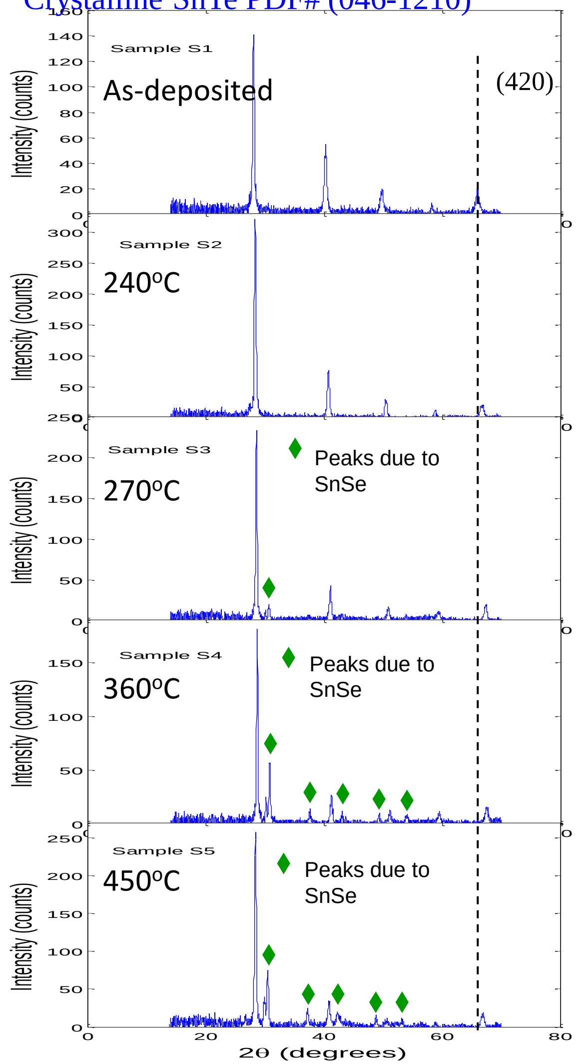

Ge2Se3/SnTe

- **Measured *d* spacings are affected by residual stress and temperature dependent compositional changes**

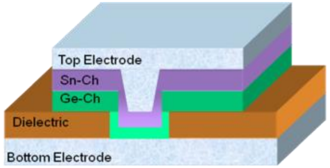

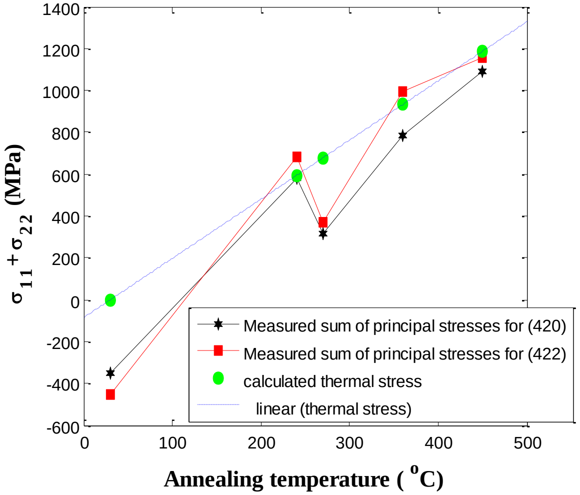

- 180°C – 240°C: Gradual decrease in d_{200}
- 240°C – 330°C: Sharp decrease in d_{200} – separation of SnSe phase
- 330°C – 450°C: Decrease and then increase in d_{200}
  - At 360°C – possibility of second phase transition

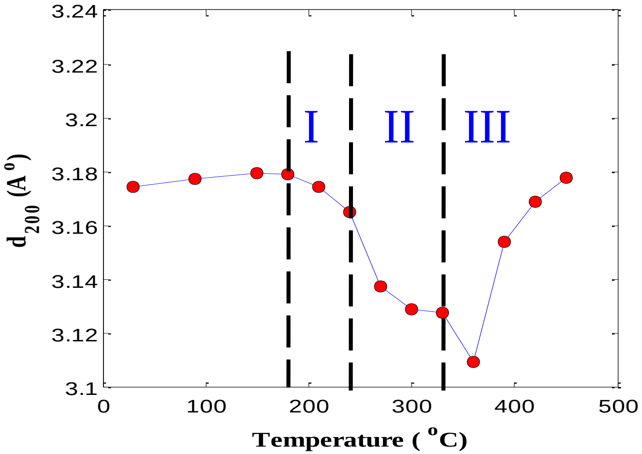

Ge_2Se_3/SnTe

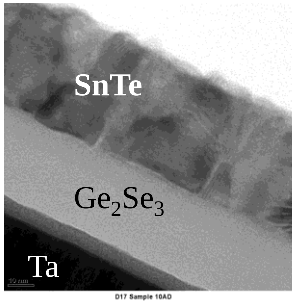

Annealed to 200°C

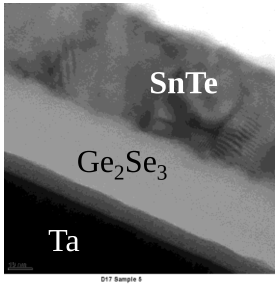

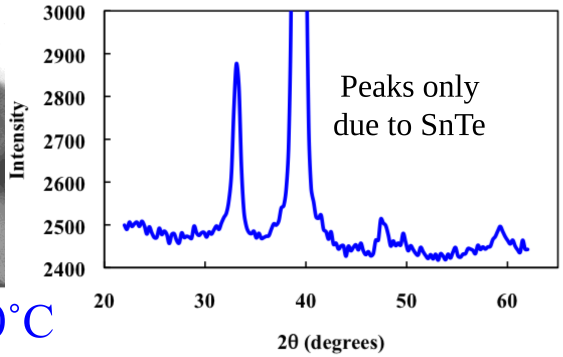

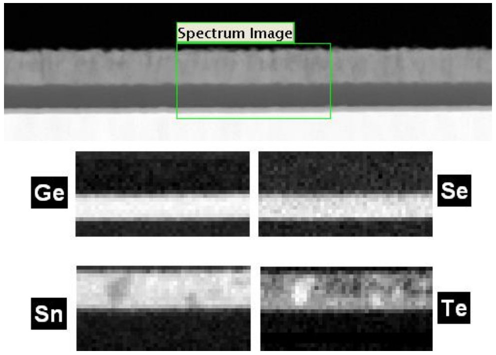

Annealed to 550°C

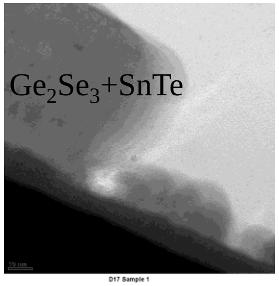

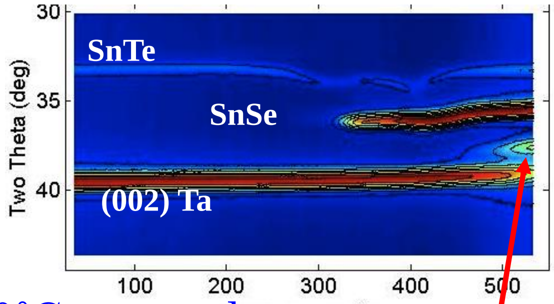

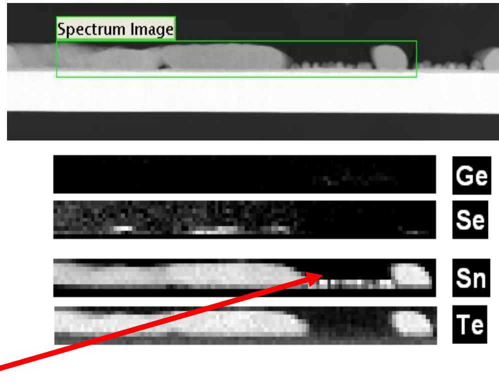

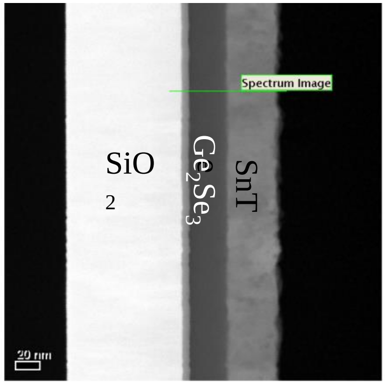

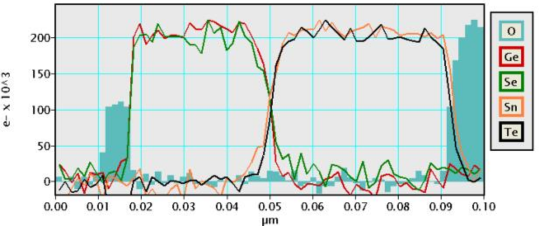

Annealed to 600°C - capped

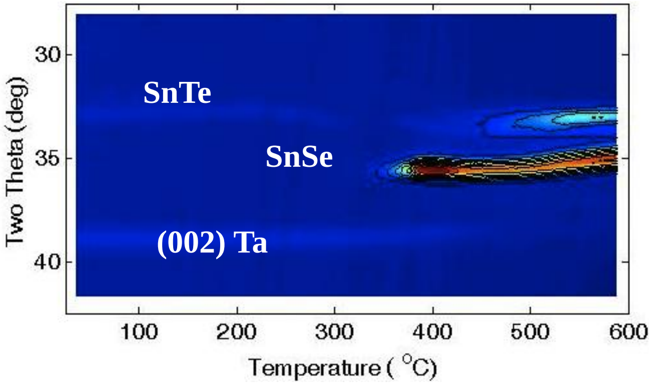

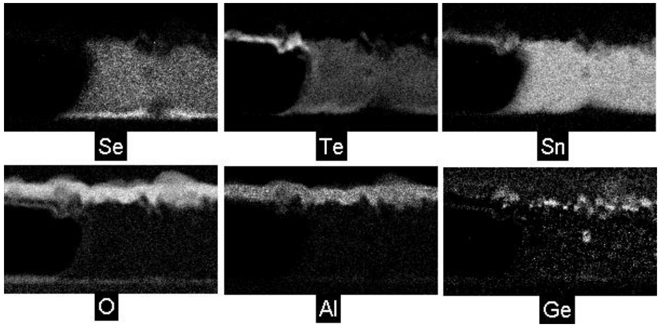

GeTe/SnTe Bilayer

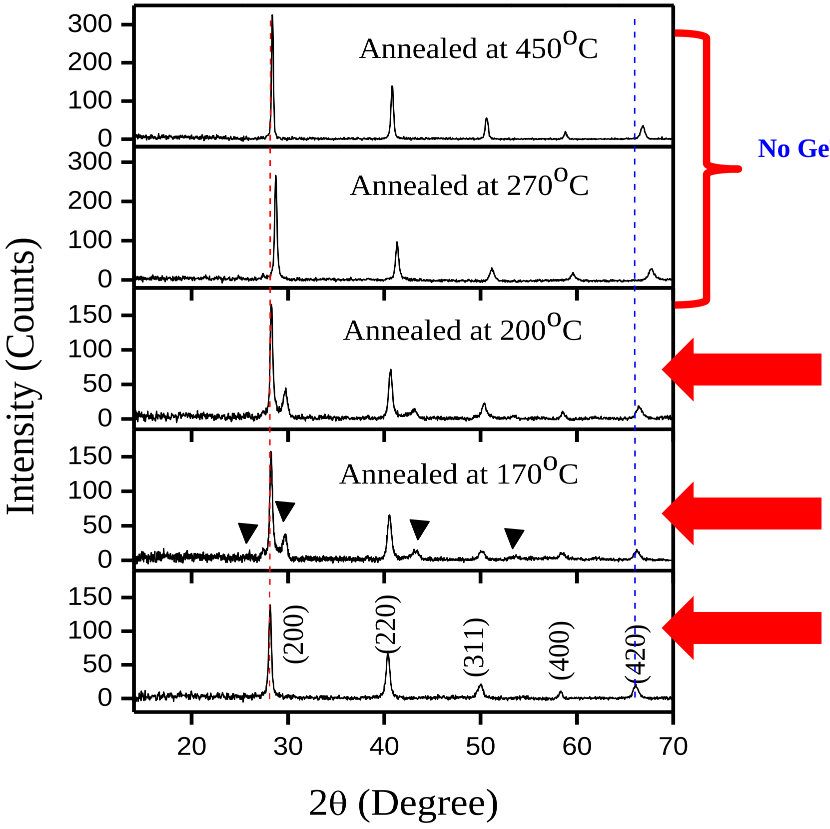

No GeTe peaks

stronger GeTe peaks
(420) Right shift

GeTe (PDF # 052-0849) phase separation
(420) Right shift

Amorphous GeTe
Crystalline SnTe (PDF# 046-1210)

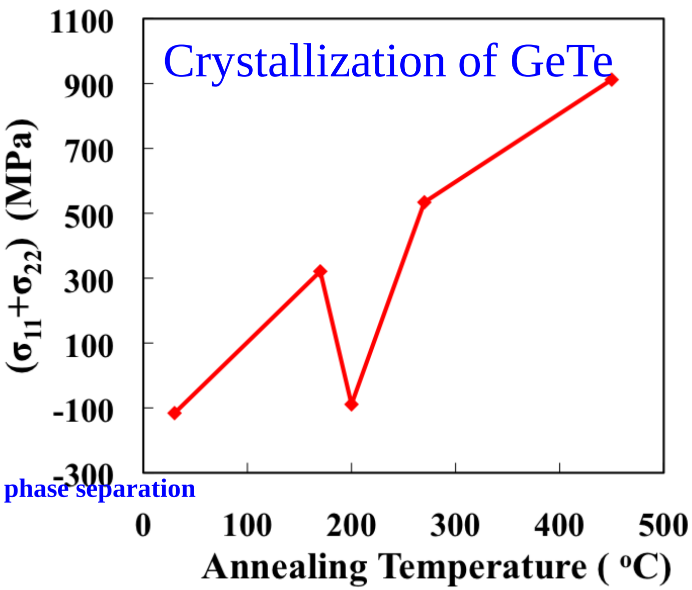

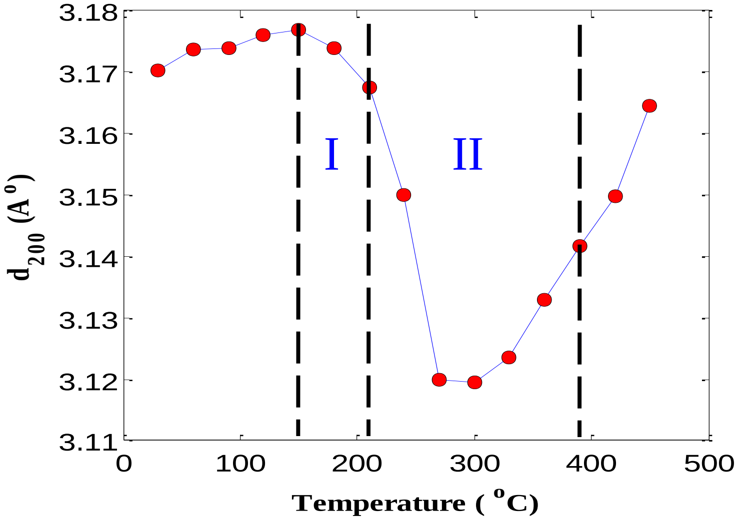

- 170°C – 210°C: Gradual decrease in d_{200} – crystallization of GeTe
- 210°C – 400°C: Decrease and then increase in d_{200} – possibility of formation of GeTe – SnTe solid solution

TRXRD at NSLS, BNL

GeTe/SnSe

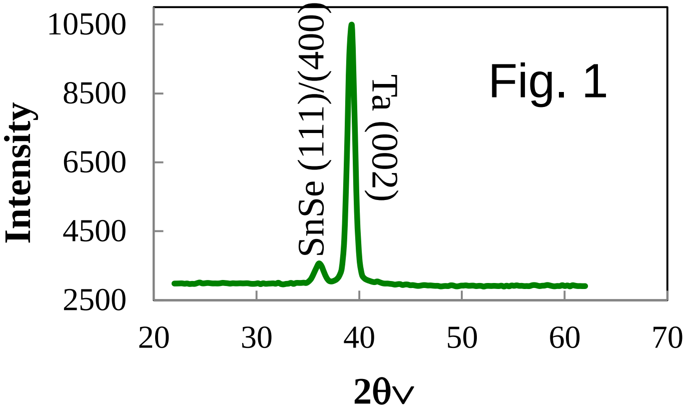

Fig. 1

As-deposited Amorphous GeTe

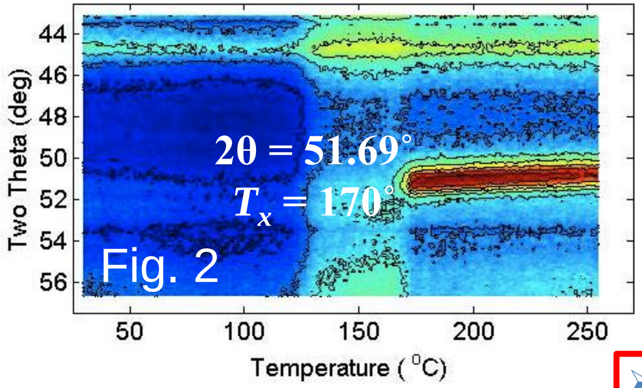

$2\theta = 51.69^\circ$
$T_x = 170^\circ$

Fig. 2

Annealed to 270°C
GeTe crystallization
(PDF# 471079)

rhombohedral to cubic shift from $2\theta = 35.14^\circ$ to $2\theta = 33.95^\circ$

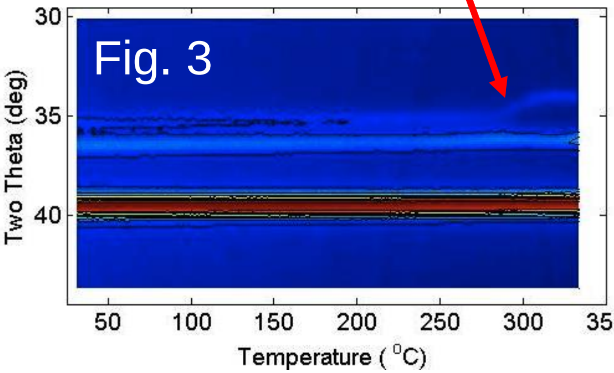

Fig. 3

Annealed to 340°C

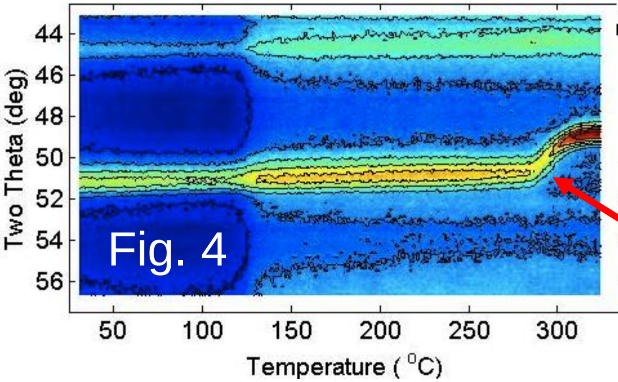

Fig. 4

rhombohedral to cubic shift from $2\theta = 51.69^\circ$ to $2\theta = 49.49^\circ$

Annealed to 550°C

$2\theta = 37.44^\circ$ $TaTe_2$ or Sn?

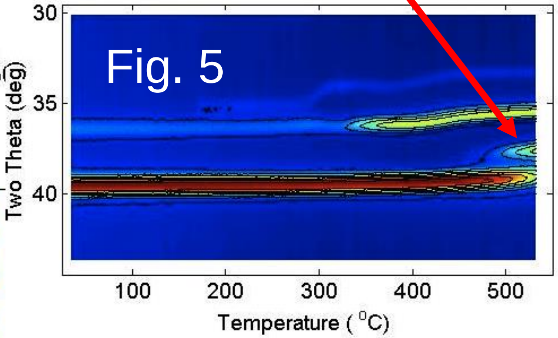

Fig. 5

- **Sn incorporation from top layer**
- **Formation of $Ge_{1-x}Sn_xTe$ solid solution**
- **Decrease in rhombohedral to cubic transition temperature to 290°C – 300°C**

GeTe/SnSe

As-deposited

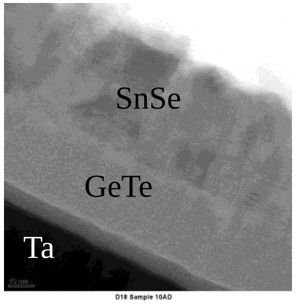

Annealed to 340°C

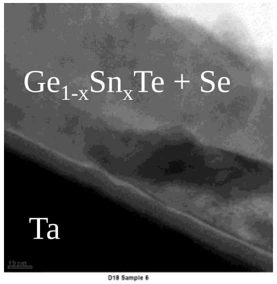

Rhombohedral to cubic shift

@ 300°C – $Ge_{1-x}Sn_xTe$

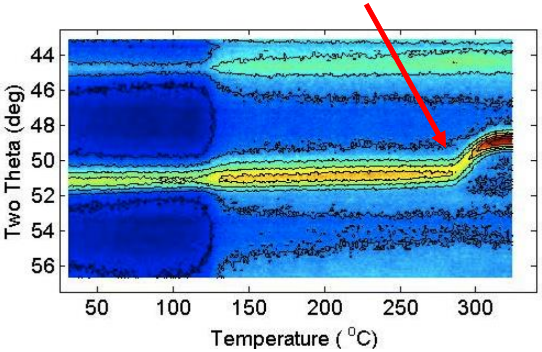

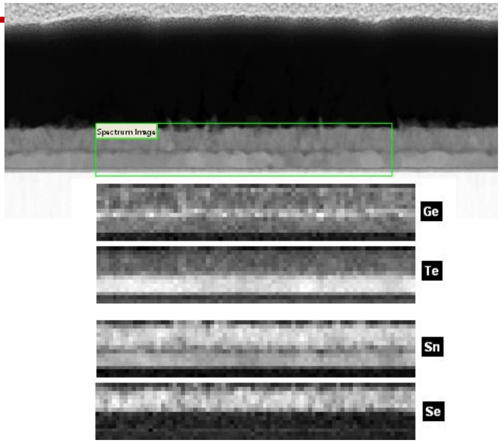

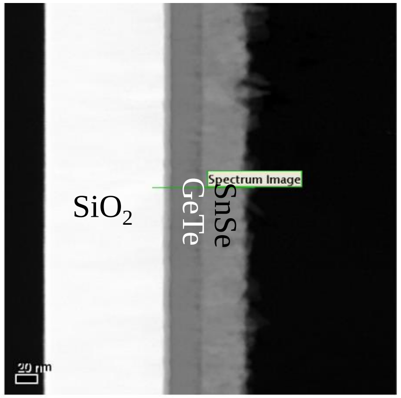

Annealed to 550°C

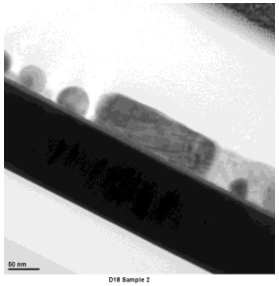

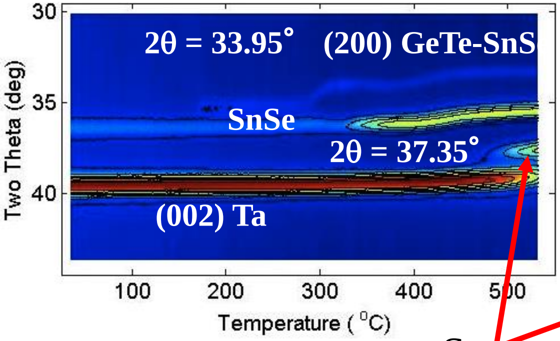

Sn

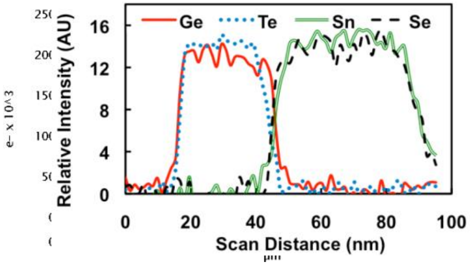

Annealed to 600°C - capped

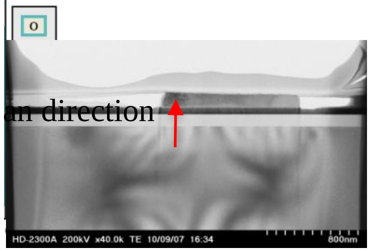

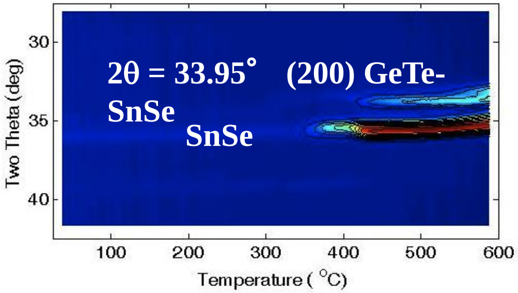

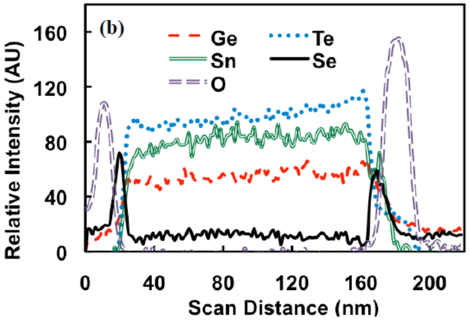

Results Summary

As deposited XTEM

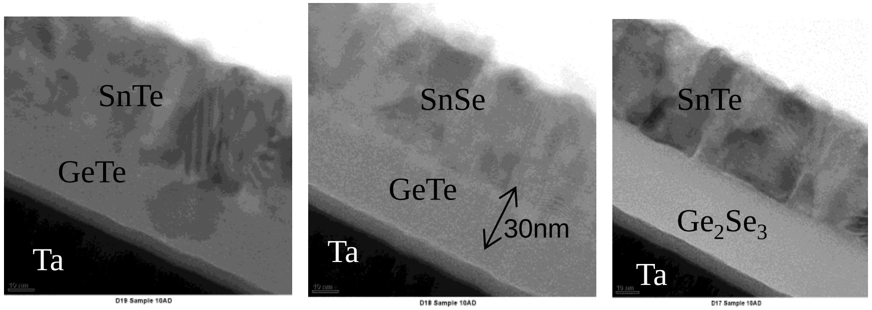

Ge-Ch Amorphous; Sn-Ch Crystalline

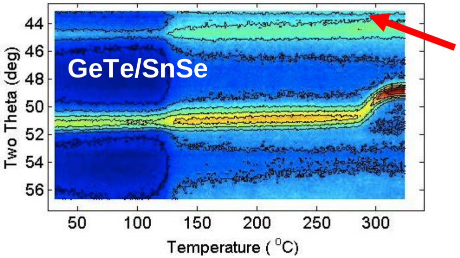

Rhombohedral to cubic shift ~ 300C

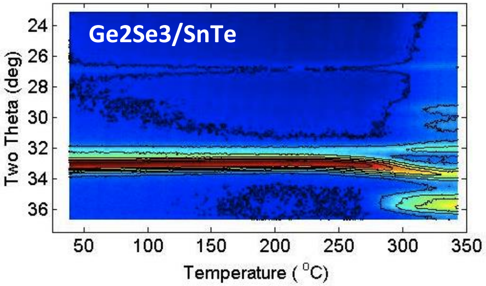

Sn incorporation from top layer reduces crystallization temperature from 430˚C

Summary

Bilayer	Effective Threshold Field V/µm	Current Density at Threshold µA µm^{-2}	Resistance ON/OFF Ratio	Crystallization and Structural Transition Temperature ºC
GeTe/SnTe	25	3	10^{-5}	170
GeTe/SnSe	64	110	10^{-2}	170/ 300
Ge_2Se_3/SnTe	40	0.75	10^{-5}	300-350
Ge_2Se_3/SnSe	71	95	10^{-3}	300-350

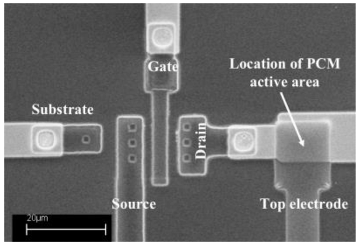

MOS Connected PCM

Electrical Data

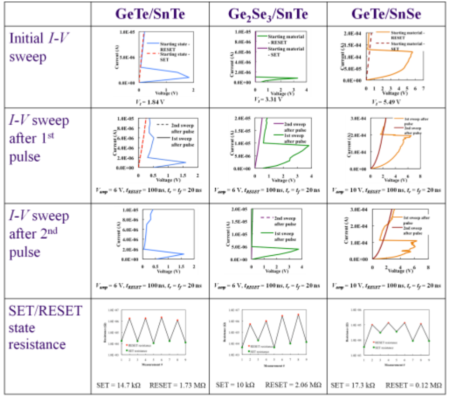

	GeTe/SnTe	Ge_2Se_3/SnTe	GeTe/SnSe
Initial *I-V* sweep	V_t = 1.84 V	V_t = 3.31 V	V_t = 5.49 V
I-V sweep after 1st pulse	V_{amp} = 6 V, t_{RESET} = 100ns, $t_r = t_f$ = 20 ns	V_{amp} = 6 V, t_{RESET} = 100ns, $t_r = t_f$ = 20 ns	V_{amp} = 10 V, t_{RESET} = 100 ns, $t_r = t_f$ = 20 ns
I-V sweep after 2nd pulse	V_{amp} = 6 V, t_{RESET} = 100ns, $t_r = t_f$ = 20 ns	V_{amp} = 6 V, t_{RESET} = 100ns, $t_r = t_f$ = 20 ns	V_{amp} = 10 V, t_{RESET} = 100 ns, $t_r = t_f$ = 20 ns
SET/RESET state resistance	SET = 14.7 kΩ RESET = 1.73 MΩ	SET = 10 kΩ RESET = 2.06 MΩ	SET = 17.3 kΩ RESET = 0.12 MΩ

Conclusions

- Threshold voltage can be tailored by the choice of Sn-chalcogenide
- Sn ions lower the crystallization temperature of Ge-chalcogenides
- Interdiffusion studies reveal the temperature limitations of each bilayer stack on processing
- Inclusion of SnTe shows higher endurance

Bilayer	T_x	Potential Application
GeTe/SnTe	170˚C	Consumer electronics
GeTe/SnSe	170˚C – phase transition 300˚C – structural transition	Consumer electronics Multi-bit applications
Ge_2Se_3/SnTe	300˚C	Automotive

Doped GST and GeTe

- Co-sputtering from Alloy Targets
- Composition determined by Rutherford Backscattering Spectroscopy (RBS) And Particle Induced X-ray Emission (PIXE)

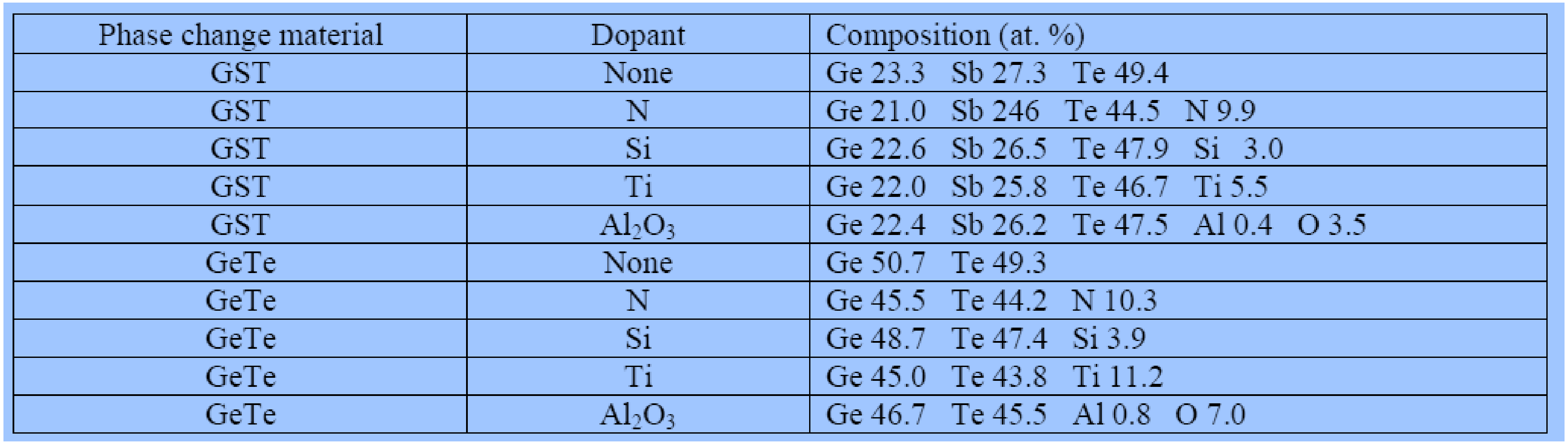

Phase change material	Dopant	Composition (at. %)
GST	None	Ge 23.3 Sb 27.3 Te 49.4
GST	N	Ge 21.0 Sb 246 Te 44.5 N 9.9
GST	Si	Ge 22.6 Sb 26.5 Te 47.9 Si 3.0
GST	Ti	Ge 22.0 Sb 25.8 Te 46.7 Ti 5.5
GST	Al_2O_3	Ge 22.4 Sb 26.2 Te 47.5 Al 0.4 O 3.5
GeTe	None	Ge 50.7 Te 49.3
GeTe	N	Ge 45.5 Te 44.2 N 10.3
GeTe	Si	Ge 48.7 Te 47.4 Si 3.9
GeTe	Ti	Ge 45.0 Te 43.8 Ti 11.2
GeTe	Al_2O_3	Ge 46.7 Te 45.5 Al 0.8 O 7.0

TRXRD on Doped GST and GeTe

- Time resolved x-ray diffraction at Brookhaven National Lab
  - Intensity of diffracted peaks at a ramp of 1 °C/s to 450 °C.
  - Shows transition from amorphous to crystalline phase

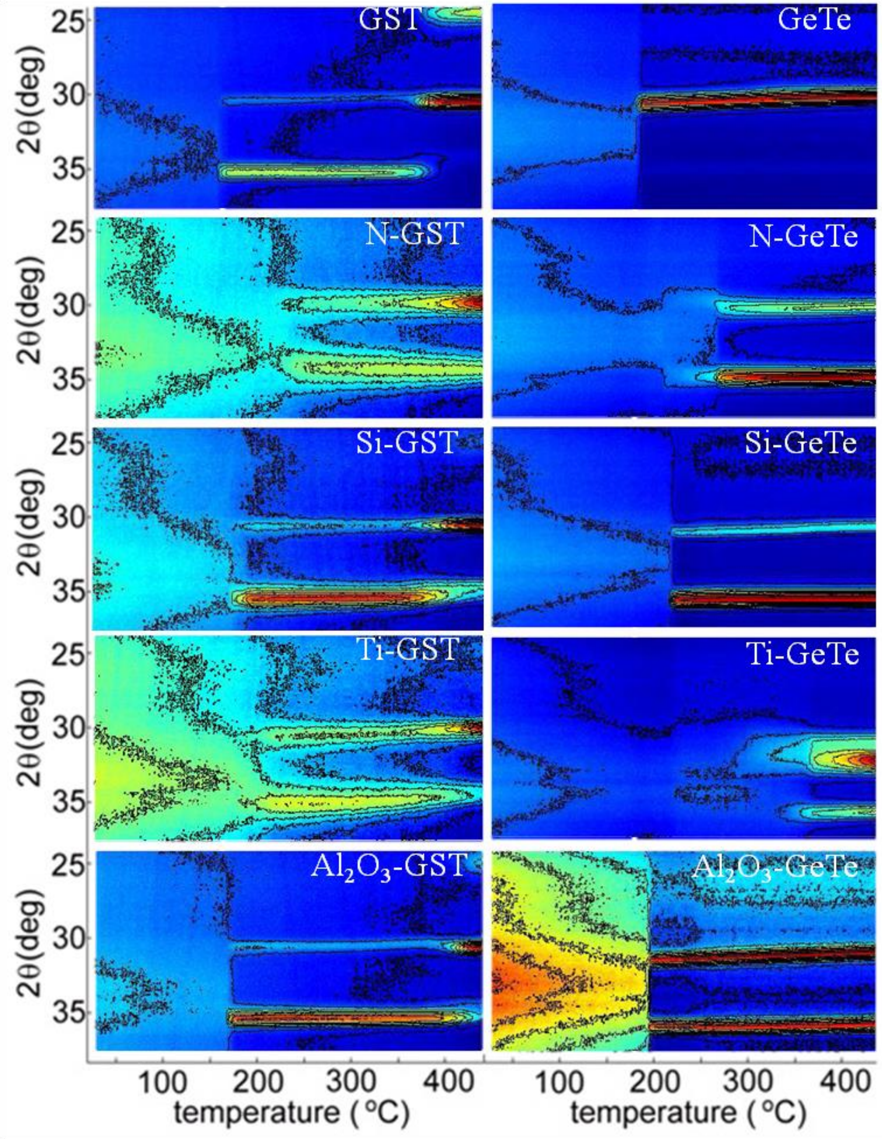

Influence of Dopants on the Crystallization Temperature, Crystal Structure, Resistance, and Threshold Field for GeTe and $Ge_2Sb_2Te_5$ Phase Change Materials, S. Raoux, D. Cabrera, A. Devasia, S. Kurinec, H. Cheng, Y. Zhu, C. Breslin and J. Jordan-Sweet, European\Phase Change and Ovonics Symposium, September 2011, Zurich, Switzerland.

- θ to 2θ scans after temperature ramp shows phase transition

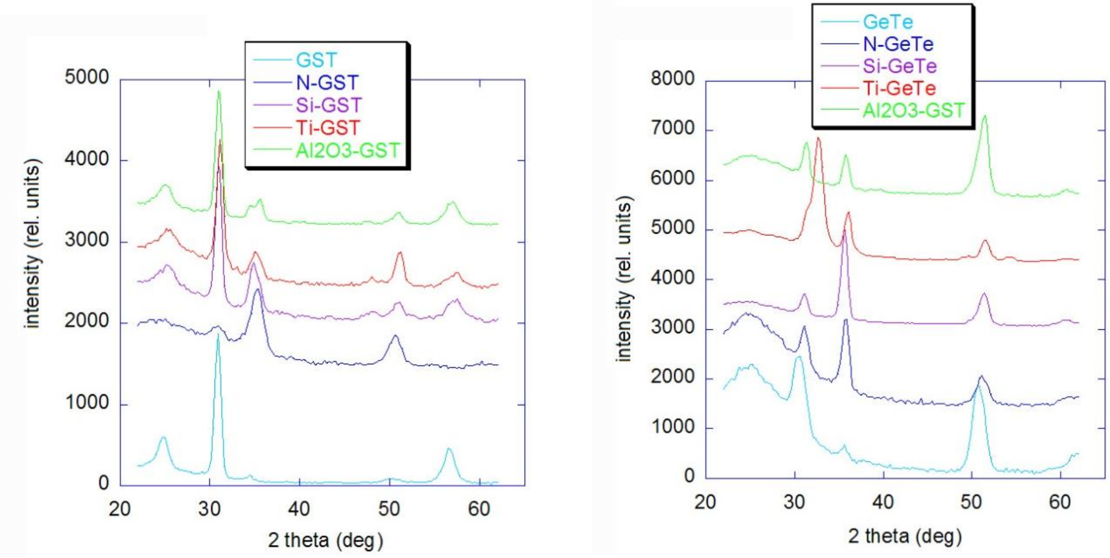

- Resistivity as a function of temperature shows resistance change as material crystallizes

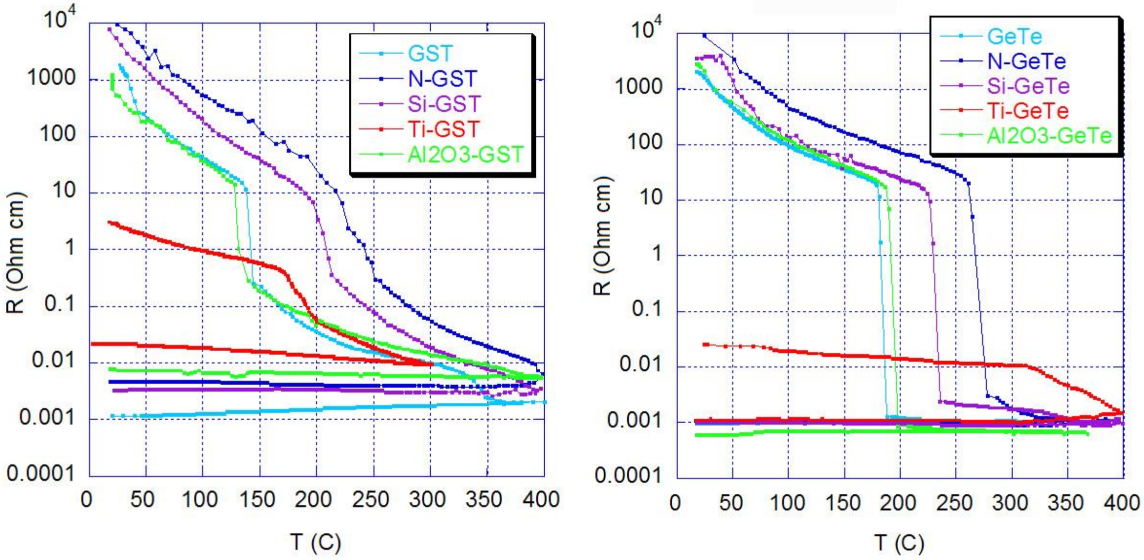

Effect of Dopants on Crystallization & Threshold Field

- It was concluded that dopants raise chalcogenide crystallization temperature.
- Nitrogen dopant was the most effective, raising GeTe to 270 °C compared to undoped at 170 °C.

	XRD (°C)
GST	**160**
NGST	**230**
TiGST	**200**
SiGST	**175**
AlO_2GST	**170**

GeTe	**180**
NGeTe	**270**
TiGeTe	**220**
SiGeTe	**220**
AlO_2GeTe	**200**

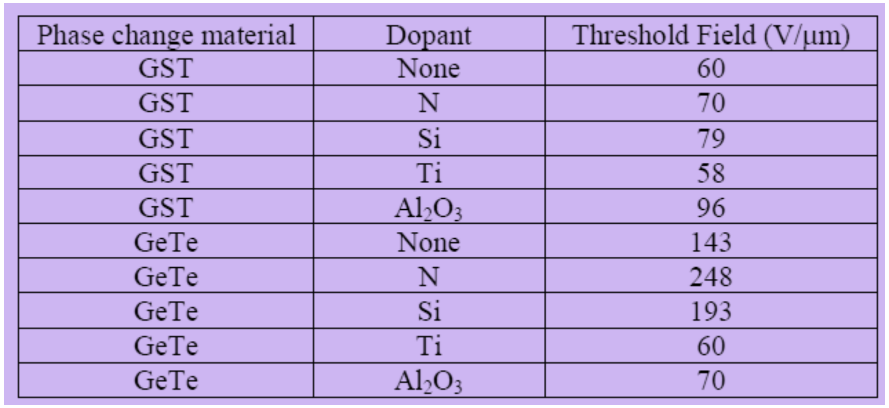

Phase change material	Dopant	Threshold Field (V/µm)
GST	None	60
GST	N	70
GST	Si	79
GST	Ti	58
GST	Al_2O_3	96
GeTe	None	143
GeTe	N	248
GeTe	Si	193
GeTe	Ti	60
GeTe	Al_2O_3	70

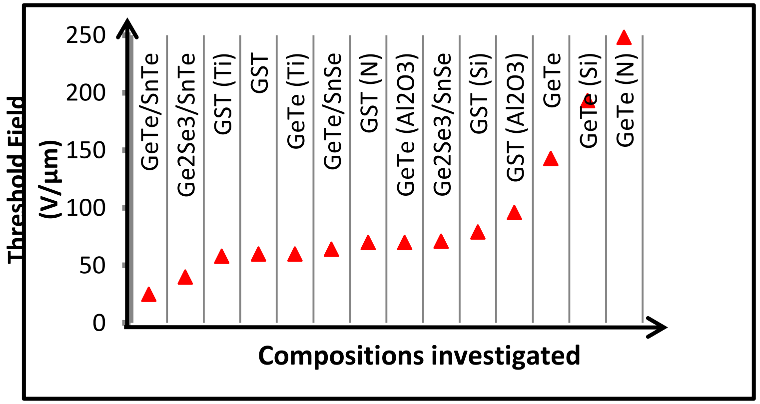

Fig.1 Threshold fields achieved for different material compositions

High threshold fields are desirable for ultra-scaled devices because for a very small size of the amorphous region, the threshold voltage might become comparable to the reading voltage and the reading operation would disturb the state of the cell.

Evolution of Phase Change Materials

Material	Characteristics
GST	Most widely researched, only single-bit operation possible
Bilayers of Ge-Ch/Sn-Ch	Tunable phase transition characteristics, superior adhesion to electrodes, possibility of multi-bit operation
GST or GeTe with Si, SiO_2, N or Ge dopants	Reduction in programming current, faster crystallization, improved thermal stability of crystalline phase
GST, AIST, GeSe, GeTe nanoparticles	Potential for scaling to very small dimensions, cost reduction by means of self-assembly and spin-on techniques

Metrology & Characterization Indispensable

More and more new materials are being introduced in emerging memory technologies

State of the Art Tools

Research on

  *New Techniques

Education

  *Metrology

  *SPC

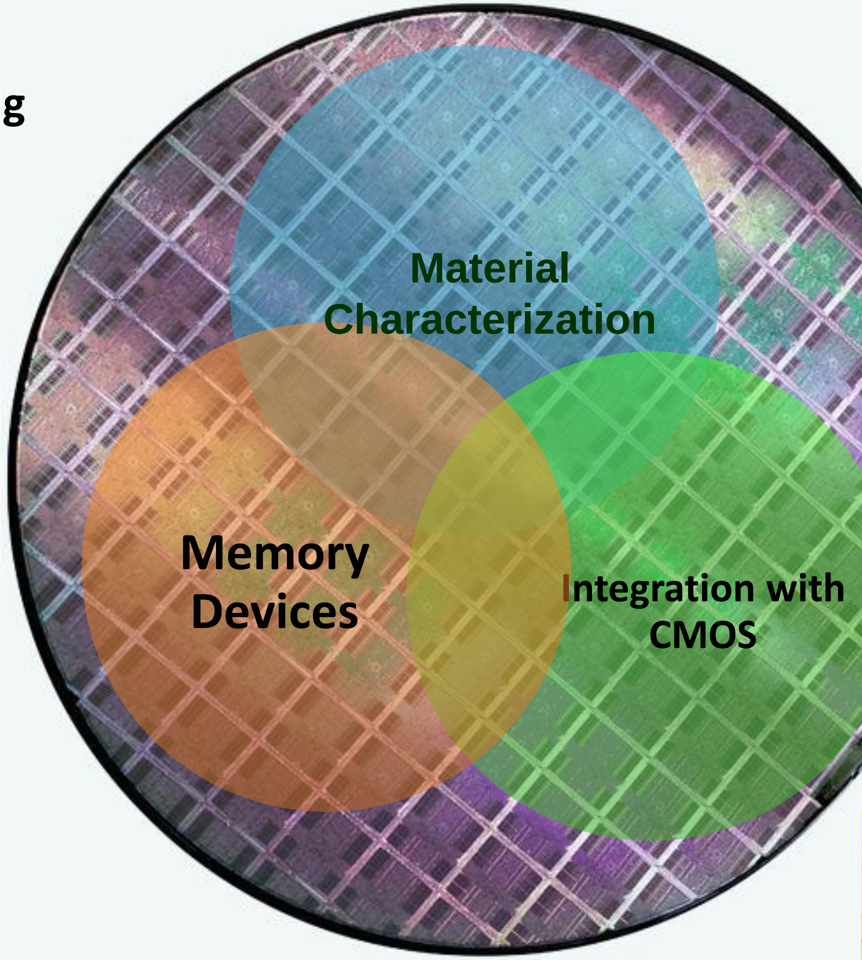

Material Characterization

Memory Devices

Integration with CMOS

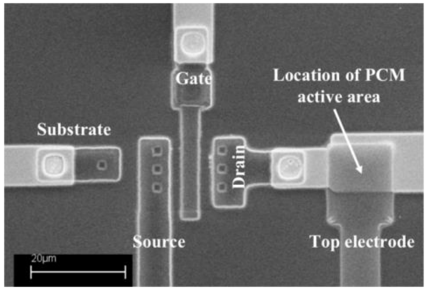

Acknowledgments

This work was supported in part by the NSF grant ECCS-0501460 and EEC-0530575.

NASA EPSCoR Grant # NNX07AT60A

National Synchrotron Light Source, Brookhaven National Laboratory, supported by the U.S. DOE, Contract # DE-AC02- 98CH10886

Chih-Ling Lee, Katrina Rook, Narsima Srinivasan, and Ramya Chandrasekaran (Veeco)